

AD-A112 631

ARMY ELECTRONICS RESEARCH AND DEVELOPMENT COMMAND WS--ETC F/6 20/7  
PROPERTIES OF DUST AS AN ELECTRON AND ION ATTACHMENT SITE FOR U--ETC(U)  
OCT 81 H P COLE, M G HEAPS

UNCLASSIFIED

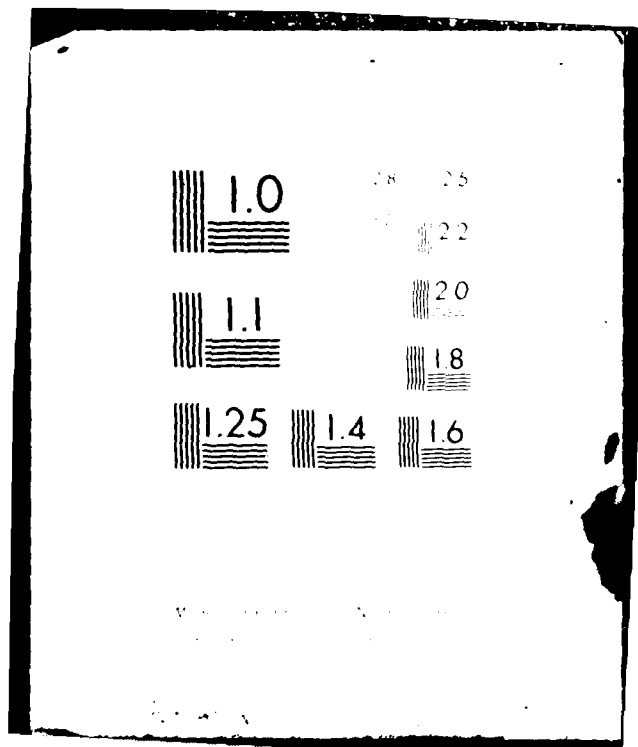
ERADCOM/ASL-TR-0098

NL

1 OF 1  
AD-A  
20/7

01

END  
DATE  
04-82  
DTIC





-TR-0098

12

AD

Reports Control Symbol  
OSD - 1366

AB AL 112631

PROPERTIES OF DUST AS AN ELECTRON AND ION ATTACHMENT  
SITE FOR USE IN D REGION ION CHEMISTRY

OCTOBER 1981

By

**Henry P. Cole**  
National Research Council Research Associate  
US Army Atmospheric Sciences Laboratory  
White Sands Missile Range, New Mexico 88002

**Melvin G. Heaps**  
US Army Atmospheric Sciences Laboratory  
White Sands Missile Range, New Mexico 88002

DTIC  
SELECTED  
MAR 30 1982  
S D  
B

Approved for public release; distribution unlimited.



US Army Electronics Research and Development Command  
**Atmospheric Sciences Laboratory**  
White Sands Missile Range, NM 88002

## NOTICES

### Disclaimers

The findings in this report are not to be construed as an official Department of the Army position, unless so designated by other authorized documents.

The citation of trade names and names of manufacturers in this report is not to be construed as official Government endorsement or approval of commercial products or services referenced herein.

### Disposition

Destroy this report when it is no longer needed. Do not return it to the originator.

SECURITY CLASSIFICATION OF THIS PAGE (When Data Entered)

20. ABSTRACT (cont)

establishes some basic properties of single particulates such as the electron-particulate and ion-particulate attachment rates, recombination rates, and photodetachment rates. A derivation of attachment coefficients for particulates acting en masse in the D region plasma is next examined. The limitations to this approach are outlined along with a discussion of preferred charge loading distributions on the particulates under various ambient conditions. Finally, illustrative examples are given of the effect of particulates on D-region electron density profiles and charge balance.

## CONTENTS

LIST OF FIGURES.....	4
LIST OF TABLES.....	4
NOTATIONS.....	5
1. INTRODUCTION.....	7
2. PROPERTIES OF MESOSPHERIC PARTICLES.....	9
3. ELECTRON AND ION ATTACHMENT TO SINGLE DUST PARTICLES.....	11
4. EFFECTIVE CHARGE ATTACHMENT COEFFICIENTS.....	14
4.1 Derivation.....	14
4.2 Choice of Photodetachment Coefficient for Dust.....	17
4.3 Charge Loading on Dust.....	19
4.4 Effective Dust Attachment Coefficients.....	24
5. THE EFFECTS OF DUST ON D REGION CHEMISTRY AND CHARGE BALANCE THROUGH THE USE OF A FULL CHEMICAL CODE.....	25
5.1 Runs at 80 km with Variable Dust Concentration and Photodetachment.....	25
5.2 Comparison of the Effects of Four Dust Profiles ( $r = 0.01\mu\text{m}$ and $r = 0.001\mu\text{m}$ ) upon D-region Ion Chemistry .....	27
6. SUMMARY AND CONCLUSIONS.....	28
REFERENCES.....	31

RE: ASL-TR-0098, Classified  
References, Distribution Unlimited  
No change in distribution statement  
per Mr. Buck Sims, AASL/DELAS-~~DM~~-A.

Accession For  
MILITARY  
TECHNICAL  
DATA  
AS  
AND  
SPECIAL  
CLASSIFICATION  
DISTRIBUTION  
AVAILABILITY CODES  
AVAIL AND/OR  
DIST SPECIAL  
**A**

## LIST OF FIGURES

1. A plot of the capture rate modification function (F) against the absolute charge, Z, on a dust particle of radius 0.1 $\mu$ m to 0.001 $\mu$ m.....	12
2. A plot showing the magnitude of $k_D^e$ , the dust-electron attachment coefficient (left ordinate), for various radii dust of charge Z = -1, 0, +1.....	15
3. A plot showing the magnitude of $\nu_D^e$ , the dust-electron attachment frequency (left ordinate), for various radii dust of charge Z = -1, 0, +1.....	20
4. Values of the effective attachment coefficients of 0.001 $\mu$ m and 0.01 $\mu$ m dust to electrons, $k_D^e$ , and positive ions, $k_D^+$ , for populations of electrons and ions.....	23
5. A plot of observed electron densities.....	29

## LIST OF TABLES

1. $k_D^e$ AND $k_D^+$ , ELECTRON AND POSITIVE ION ATTACHMENT COEFFICIENTS FOR A SINGLE DUST PARTICLE AT T = 150°K.....	13
2. PERCENT OF DUST POPULATION WITH A PARTICULAR NUMBER OF ELECTRONS FOR T = 150°K.....	21
3. VARIATION IN ELECTRON DENSITY AT 80 km DUE TO VARIABLE DUST CONCENTRATION AND PHOTODETACHMENT.....	26
4. SELECTED DUST PROFILES.....	27

### NOTATIONS

$a$	Radius of dust particles, centimeters
$z$	Number of electronic charges on dust, a positive or negative integer
$e$	Electronic charge
$T$	Absolute temperature
$\bar{C}$	Mean thermal speed of ions or electrons. For ions, assume a mass of 50 amu. Therefore $\bar{C}_+ \approx 2.6 \times 10^5 \text{ cm s}^{-1}$ . For electrons, $\bar{C}_e \approx 300 \bar{C}_+$ .
$F$	Geometric modification shape factor
$N_e$	Number density of electrons, centimeter <sup>-3</sup>
$N_+$	Number density of positive ions, centimeter <sup>-3</sup>
$N_-$	Number density of negative ions, centimeter <sup>-3</sup>
$N_D$	Number density of dust, centimeter <sup>-3</sup>
$v_z$	Frequency of capture of positive ions by dust particles with a charge $z$ , second <sup>-1</sup>
$v_z^e$	Frequency of capture of electrons by dust particles with a charge $z$ , second <sup>-1</sup>
$v_z^-$	Frequency of capture of negative ions by dust particles with a charge $z$ , second <sup>-1</sup>
$v_{ph}$	Photodetachment frequency, second <sup>-1</sup>
$p_z$	Fraction of dust particles which carry a charge $z$
$k_D^e$	Coefficient of attachment of an electron to a single dust particle, centimeter <sup>3</sup> second <sup>-1</sup>
$k_D^+$	Coefficient of attachment of a positive ion to a single dust particle, centimeter <sup>3</sup> second <sup>-1</sup>
$k_D^e$	Effective attachment coefficient of electrons in a distribution of dust particles, centimeter <sup>3</sup> second <sup>-1</sup>
$k_D^+$	Effective attachment coefficient of positive ions in a distribution of particles, centimeter <sup>3</sup> second <sup>-1</sup>

## 1. INTRODUCTION

The D region is the lowest portion of the ionosphere and nominally encompasses the altitude range of 60 to 90 km. It represents a transition region for the ionospheric plasma composition. Above 80 to 85 km, daytime composition is limited to molecular ions such as  $\text{NO}^+$  and  $\text{O}_2^+$ ; while below 80 to 85 km, the simple molecular ions enter into clustering reactions which convert the positive ion composition into one dominated by water clusters. Electrons also undergo attachment processes in the D region to form negative ions; by day this attachment appears to take place below 70 to 75 km. By night it occurs as high as 90 km, but there are still many unanswered questions concerning the negative ion chemistry.

The sources of ionization within the D region are the "tail end" of the solar x-ray spectrum, mainly at wavelengths less than 1 nm and in the 3- to 10-nm range, and two strong solar emission lines, Lyman beta at 102.6 nm which ionizes  $\text{O}_2$  and Lyman alpha at 121.6 nm which ionizes NO. Ionization from these sources occurs principally above 75 km. Below 70 km galactic cosmic rays are the main (though small) source of ionization. At higher latitudes charged particle precipitation and associated bremsstrahlung x-rays may occasionally be the dominant ionization source.

The deposition of micrometeors, at the altitude of the lower portion of the E region and upper portion of the D region, produces a concentration of metallic ion layers at 90 to 110 km and occasional occurrences of sporadic E reflection. Estimates have shown that this micrometeor flux may be sufficiently large to serve as source material for the mesospheric scattering layers and noctilucent clouds which are often observed in the 80 to 85 km range.<sup>1</sup>

Certain D region phenomena have been observed which have no ready explanation in terms of conventional ion chemistry; for example, electron density profiles have occasionally shown layers of sharply decreased concentration in the 80 to 90 km range, which could be interpreted as due to particulate layers which have the ability to attach electrons.<sup>2</sup> This ability would suggest, therefore, that there is a large group of primarily negatively charged species, either

---

<sup>1</sup>D. M. Hunten, R. P. Turco, and O. B. Toon, 1980, "Smoke and Dust Particles of Meteoric Origin in the Mesosphere and Stratosphere," J Atmos Sci, 37:1342.

<sup>2</sup>A. Pedersen, J. Troin, and J. A. Kane, 1970, "Rocket Measurements showing a Removal of Electrons Above the Mesopause in Summer at High Latitude," Planet Space Sci, 18:945-947.

ions or particulates, present in the upper D region.<sup>3</sup> And indeed, conductivity measurements throughout the stratosphere and mesosphere give evidence of light and "massive" ions, which may be interpreted to be charged particulates. D-region electron densities observed during some solar eclipses have indicated a surprisingly rapid electron density decrease which cannot be explained on the basis of current knowledge of electron-ion rates of recombination.<sup>4</sup>

With these examples of anomalous behavior in mind, the purpose of this report is to establish properties of particulates necessary for use in particle-predictive computer codes. These properties are electron-particulate and ion-particulate collision frequencies, attachment and recombination rates, and electron photodetachment rates. To achieve this result, the coefficients will be examined on three levels: (1) Coefficients will be derived for single particles impacting with electrons or ions. (2) An "effective" or "net" attachment coefficient shall be derived which pertains to a population of dust mixed with ambient electrons and positive ions. This derivation follows the work of Parthasarathy and Rai<sup>5</sup> and Parthasarathy<sup>6</sup> but has certain limitations which shall be examined. This treatment is instructive since it derives the charge loading on a population of dust and outlines the sensitivity of the attachment coefficients to various parameters. (3) Particulates will be included and evaluated as electron or ion attachment sites within a full time-dependent chemical code which includes all other competitive processes of the region chemistry.

---

<sup>3</sup>M. G. Heaps, F. E. Niles, and R. D. Sears, 1978, Modeling the Ion Chemistry of the D-region: A Case Study Based Upon the 1966 Total Solar Eclipse, ASL-TR-0015, US Army Atmospheric Sciences Laboratory, White Sands Missile Range, NM.

<sup>4</sup>M. G. Heaps and J. M. Heimerl, 1980, "The Quiet Midlatitude D-region: A Comparison Between Modeling Efforts and Experimental Efforts," J Atmos Terr Phys, 42:733.

<sup>5</sup>E. A. Mechtly, C. F. Sechrist, Jr., and L. G. Smith, 1972, "Electron Loss Coefficients for the D-region and the Ionosphere from Rocket Measurements During the Eclipses of March 1970 and November 1966," J Atmos Terr Phys, 34:641

<sup>6</sup>R. Parthasarathy and D. B. Rai, 1966, "Effect of Meteoric Dust on the Effective Recombination Coefficient in the Lower Ionosphere," Radio Sci, 1:1401.

<sup>7</sup>R. Parthasarathy, 1976, "Mesopause Dust as a Sink for Ionization," J Geophys Res, 81:2392.

## 2. PROPERTIES OF MESOSPHERIC PARTICLES

Noctilucent clouds (NLC) have long provided the most direct and visual evidence that particulates, most likely pure ice or ice coated dust, tend to layer at the summer mesopause. The rare observation of NLC during stratospheric warmings indicates layering in winter also.<sup>9</sup> OGO-6 satellite observations<sup>10</sup> indicate that particulate layers near the 82 km upper bound of the mesosphere may be a persistent high latitude feature, while global lidar observations show a sodium layer in this same region. Witt<sup>11</sup> and Fogle and Rees<sup>12</sup> have calculated NLC particulate sizes to be of the order of 0.1 $\mu$ m to 0.2 $\mu$ m in radius with number densities of the order of 1 cm<sup>-3</sup>. Donahue et al<sup>13</sup> also estimate that 0.13 $\mu$ m radius particles with number densities of 15 to 40 cm<sup>-3</sup> would successfully explain their scattering observations. An earlier work by Divari<sup>14</sup> based upon rocket samples states that particulate concentrations in the mesosphere are an inverse function of size down to 0.05 $\mu$ m. Also model calculations by Hunten et al<sup>15</sup> indicate a similar inverse size and concentration relationship in the 80- to 90-km altitude range for particles less than 0.001 $\mu$ m.

There are three alternatives for the origin of NLC particulates: (1) They are terrestrial and ascend by the action of turbulence, (2) they are formed from in-situ ion clusters, or (3) they are meteoritic.

The first possibility seems unlikely considering the insufficient magnitude of the eddy diffusion coefficient in the stratosphere and mesosphere (see, for example, Hunten<sup>16</sup>). As for the second possibility, Witt<sup>17</sup> proposed that water

<sup>9</sup>R. A. Hamilton, 1964, "Observations of Noctilucent Clouds Near Midwinter," Met Mag Lond, 93:201.

<sup>10</sup>T. M. Donahue, B. Guenther, and J. E. Blamont, 1972, "Noctilucent Clouds in the Daytime: Circumpolar Particulate Layers Near the Summer Mesopause," J Atmos Sci, 29(6):1205.

<sup>11</sup>G. Witt, 1960, "Polarization of Light From Noctilucent Clouds," J Geophys Res, 65:925-933.

<sup>12</sup>B. Fogle and M. Rees, 1972, "Spectral Measurements of Noctilucent Clouds," J Geophys Res, 77:720.

<sup>13</sup>G. Divari, 1964, "The Dust Concentration in the Upper Layers of the Earth's Atmosphere," Geomagnetism and Aeronomy, 4:688-692.

<sup>14</sup>D. M. Hunten, R. P. Turco, and O. B. Toon, 1980, "Smoke and Dust Particles of Meteoric Origin in the Mesosphere and Stratosphere," J Atmos Sci, 37:1342.

<sup>15</sup>D. M. Hunten, 1975, Vertical Transport in Atmospheres, Atmospheres of Earth and the Planets, D. Reidel Publishing Co., Dordrecht-Holland, pp 57-72.

<sup>16</sup>G. Witt, 1969, "The Nature of Noctilucent Clouds," Space Res, IX:157-169, North Holland Publishing Co.

cluster ions in the mesosphere<sup>15</sup> <sup>16</sup> serve as condensation or sublimation nuclei. Such a clustering mechanism has been investigated for aerosols in general.<sup>17</sup> <sup>18</sup> However, the mechanism whereby clusters of ten or fewer molecules could grow or combine to form the size of particulates nominally present in the D region (hundreds or thousands of molecules) has not yet been identified. Assisted by a model calculation, Reid<sup>19</sup> has argued that if a substratum of small particulates of nominal 0.001 $\mu$ m size exists, then the growth of ice needles of a detectable size (0.13 $\mu$ m) is possible under constraints of mesospheric temperatures and low water vapor. The idea that meteoritic dust particles could be sufficiently numerous to form layers dense enough for NLC also has been theoretically supported by Chapman and Kendall.<sup>20</sup> Hunten et al<sup>1</sup> showed that a nominal meteor flux of  $10^{-16}$  g cm<sup>-2</sup> s<sup>-1</sup> is sufficient to provide a source of particulates with sizes of the order of 0.001 $\mu$ m and number densities of  $10^3$  cm<sup>-3</sup>. Also the source of particles may be multiple and seasonally dependent as suggested by data of Clemesha et al.<sup>21</sup> Thus, mesospheric particulate sizes and their number densities can apparently range from an upper bound of 0.1 $\mu$ m radius with number densities of the order of  $10^3$  cm<sup>-3</sup> or less, to a lower bound of 0.001 $\mu$ m sized particulates with number densities on the order of  $10^3$  cm<sup>-3</sup>. This range of concentrations and sizes will be used as representative in the subsequent calculations and modeling in this report.

---

<sup>15</sup>R. D. Narcisi and A. D. Bailey, 1965, "Mass Spectrometric Measurements of Positive Ions at Altitudes From 64 to 112 Kilometers," J Geophys Res., 70:3687.

<sup>16</sup>F. Arnold and W. Joos, 1979, "Rapid Growth of Atmospheric Cluster Ions at the Cold Mesopause," Geophys Res Letters, 6:763-766.

<sup>17</sup>A. W. Castleman, Jr., 1974, "Nucleation Processes and Aerosol Chemistry," Space Sci Rev., 15:547-589.

<sup>18</sup>A. W. Castleman, Jr., 1979, "Nucleation and Molecular Clustering About Ions," Adv in Colloid and Interface Sci., 10:73-128.

<sup>19</sup>G. C. Reid, 1975, "Ice Clouds at the Summer Polar Mesopause," J Atmos Sci., 32:523.

<sup>20</sup>S. Chapman and P. C. Kendall, 1965, "Noctilucent Clouds and Thermospheric Dust: Their Diffusion and Height Distribution," Quart J Roy Met Soc., 91:115.

<sup>21</sup>D. M. Hunten, R. P. Turco, and O. B. Toon, 1980, "Smoke and Dust Particles of Meteoric Origin in the Mesosphere and Stratosphere," J Atmos Sci., 37:1342.

<sup>22</sup>B. R. Clemesha, V. W. J. H. Kirchoff, D. M. Simonich, and H. Takahashi, 1978, "Evidence of an Extra-Terrestrial Source for the Mesospheric Sodium Layer," Geophys Res Letters, 5:873-877.

### 3. ELECTRON AND ION ATTACHMENT TO SINGLE DUST PARTICLES

The first quantitative steps towards examining the properties of dust in the presence of charged particles were taken in 1960 by Natanson,<sup>22</sup> who formulated a kinetic approach to the charging of dust by electrons and ions. Parthasarathy and Rai<sup>6</sup> used Natanson's approach to derive attachment coefficients for dust particles with electrons and positive ions in the mesosphere. This work was extended by Parthasarathy<sup>7</sup> to include a probabilistic formulation of the basic equilibrium equations including an explicit photodetachment term.

A dust particle is charged when an electron or ion collides with and is captured by the particle. The capture frequency,  $\nu$ , equal to the collision frequency (with a collision efficiency of 1), may be expressed as

$$\nu = \pi a^2 N \bar{C} F \quad (s^{-1}), \quad (1)$$

where  $\pi a^2$  is the geometric cross section of the particle,  $N$  is electron or ion density,  $\bar{C}$  is mean velocity, and  $F$  is a capture rate modification function or "shape factor"<sup>7</sup> which modifies the geometric cross-section and whose value depends upon the resident charge of the particle and its radius. This shape factor,  $F$ , expresses the attractive (or repulsive) effects of charged dust particles to approaching electrons or ions (figure 1).

Several points should be noted. First, the  $F$  factor for uncharged dust particles enhances the geometric cross section, an effect which increases as the particle shrinks. This effect is due to the setting up of an image charge within the particle as the electron or ion approaches its surface. Second, powerful repulsive effects lead to a practical limit of one charge for particles of approximately  $0.01\mu m$  in size or less. For such small particles, recombination or neutralization becomes greatly enhanced as the particle becomes charged. Only for particles larger than  $0.1\mu m$  does multiple charging become probable.

<sup>22</sup>G. L. Natanson, 1960, "On the Theory of the Charging of Amicroscopic Aerosol Particles as a Result of the Capture of Gas Ions," Sov Phys Tech Phys, (English Translation), 5:538.

<sup>6</sup>R. Parthasarathy and D. B. Rai, 1966, "Effect of Meteoric Dust on the Effective Recombination Coefficient in the Lower Ionosphere," Radio Sci, 1:1401.

<sup>7</sup>R. Parthasarathy, 1976, "Mesopause Dust as a Sink for Ionization," J Geophys Res, 81:2392

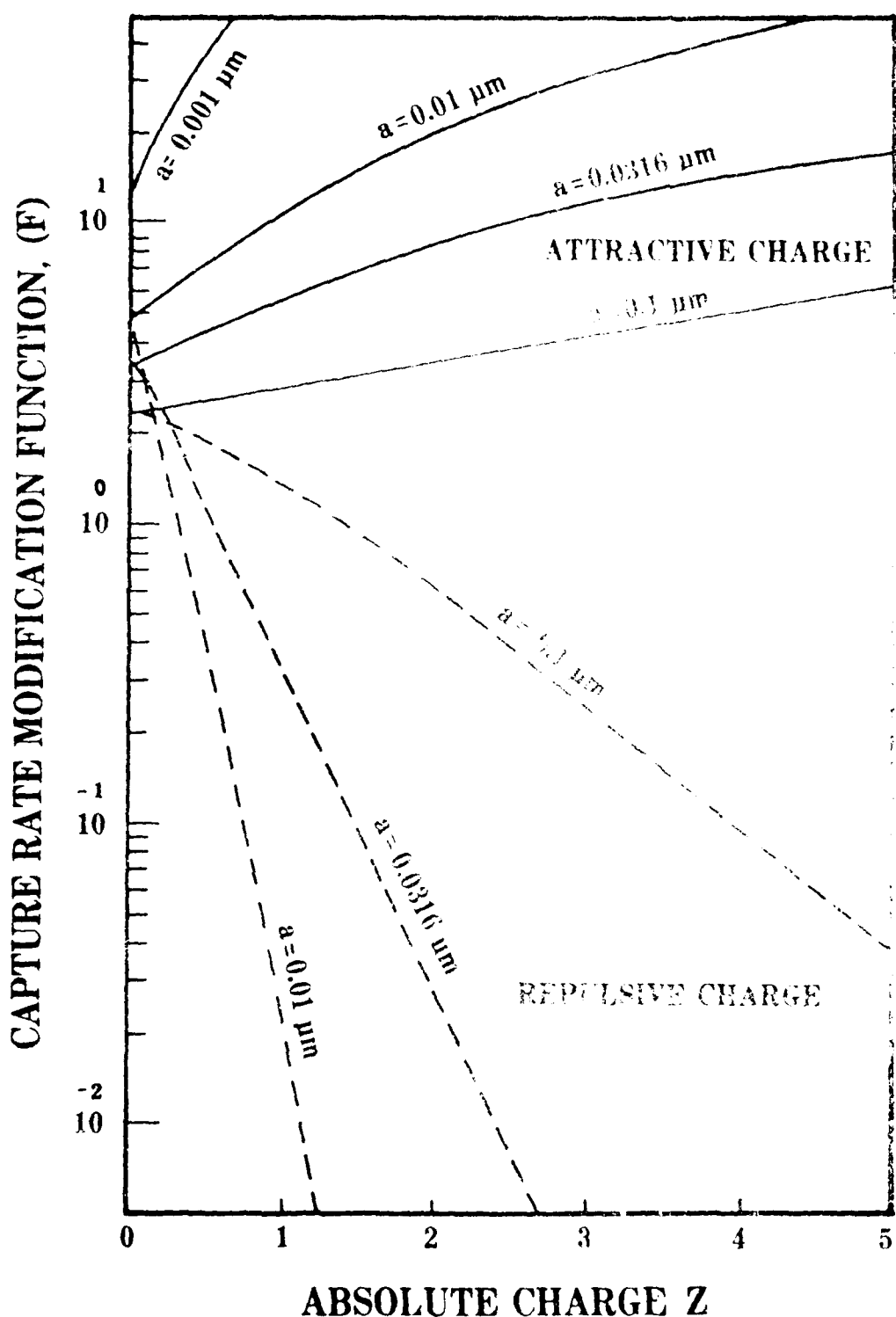


Figure 1. A plot of the capture rate modification function ( $F$ ) against the absolute charge,  $Z$ , on a dust particle of radius  $0.1\mu\text{m}$  to  $0.001\mu\text{m}$ . The value of the capture rate modification function expresses the ratio of the "effective" capture cross section of a dust particle to the simple geometric cross section and is dependent upon electrostatic effects.

The dust charge attachment coefficient,  $k_D$ , for an isolated particle is defined as

$$k_D = v/N = \pi a^2 \bar{C} F \quad (\text{cm}^3 \text{s}^{-1}), \quad (2)$$

where  $k_D$  is a function of particle size, resident charge, electron or ion mass, and velocity.  $k_D$  is to be treated as a standard chemical rate constant, where the term in the set of continuity equations becomes  $k_D^e [N_D] [N_e]$  or  $k_D^+ [N_D] [N_+]$ . Table 1 lists representative values of the coefficients  $k_D^e$  and  $k_D^+$  for a nominal mesospheric temperature  $T = 150^\circ\text{K}$ .

Points which are apparent from table 1 are: (1) the smaller the dust, the more rapidly the electron attachment coefficient decreases with increasing negative charge, (2) the larger the particle, the greater tendency it will have to attach electrons and, hence, provide an electron sink. A single large particle (that is, radius  $>0.1\mu\text{m}$ ) is therefore as effective as several smaller particles in perturbing the charge balance.

TABLE 1.  $k_D^e$  AND  $k_D^+$ , ELECTRON AND POSITIVE ION ATTACHMENT COEFFICIENTS FOR A SINGLE DUST PARTICLE AT  $T = 150^\circ\text{K}$

Dust Radius ( $\mu\text{m}$ )	Charge (e)	$k_D^e$ ( $\text{cm}^3 \text{s}^{-1}$ )	$k_D^+$ ( $\text{cm}^3 \text{s}^{-1}$ )
Z			
0.001	+1	2.6(-5)	1.3(-33)
	0	3.3(-6)	1.0(-8)
	-1	4.2(-31)	8.4(-8)
	-2	2.3(-37)	1.6(-7)
0.01	+1	2.8(-4)	7.3(-11)
	0	1.2(-4)	3.9(-7)
	-1	2.3(-7)	9.1(-7)
	-2	1.1(-10)	1.7(-6)
0.1	+1	5.0(-3)	1.1(-5)
	0	5.5(-3)	1.7(-5)
	-1	3.4(-3)	1.5(-5)
	-2	1.3(-3)	2.4(-5)
	-3	5.2(-4)	3.2(-5)
	-4	2.1(-4)	4.0(-5)
	-5	8.3(-5)	4.9(-5)
	-6	3.3(-5)	5.7(-5)
	-7	1.3(-5)	6.5(-6)
	-8	5.2(-6)	7.4(-6)

A further insight may be provided by a plot (figure 2) comparing the magnitude of the attachment coefficients,  $k_D^e$ , for  $z = -1, 0$ , and  $+1$  charged dust, as a function of particle radius, and the electron-ion recombination coefficients for  $\text{NO}^+$  and water cluster ions. This figure shows that although normally the most important loss mechanism for electrons is recombination to cluster ions, electron attachment to particulates could be dominant if the dust number density were of the same magnitude as the ion number density and (a) dust were positively charged, (b) dust were neutral but larger than  $0.002 \mu\text{m}$ , or (c) the dust particle had a single negative charge and exceeded  $0.11 \mu\text{m}$  in radius. The inferences of dust size distribution in the mesosphere allow that there could be much dust at sizes of  $0.01 \mu\text{m}$  or smaller. In that case, the probability of mesospheric dust affecting the D-region charge balance may be considerable through the formation of an electron sink.

#### 4. EFFECTIVE CHARGE ATTACHMENT COEFFICIENTS

##### 4.1 Derivation

The previous section explicitly derived the charge attachment frequency for an isolated dust particle of a given size and a known resident charge. However, in the D region, a population of dust particles will tend to possess a distribution of charge which will be established by the competitive attachment and detachment of electrons and ions. Parthasarathy and Rai<sup>6</sup> and Parthasarathy<sup>7</sup> initially addressed the calculation of the attachment coefficients for dust "en masse." In this section we analyze the limitations of this approach but show that it provides knowledge of the resident charge distribution function of dust for various ambient conditions. Photodetachment is also included in this formulation as an explicit term, and suitable experimental values are examined.

Parthasarathy<sup>7</sup> stipulates that the equilibrium condition of dust mixed with charged species is considered to be a statistically stationary distribution. This condition is formulated by stating that the frequency at which the fraction of dust particles with a charge  $z$  is being depleted by ion capture, electron capture, and photodetachment is equal to that frequency at which the fraction of dust particles with  $z + 1$  charges are acquiring electrons or negative ions plus the frequency at which the fraction of dust particles with  $z - 1$  charges are acquiring positive charges and suffering photodetachment of electrons (after Parthasarathy<sup>7</sup>).

---

<sup>6</sup>R. Parthasarathy and D. B. Rai, 1966, "Effect of Meteoric Dust on the Effective Recombination Coefficient in the Lower Ionosphere," Radio Sci., 1:1401.

<sup>7</sup>R. Parthasarathy, 1976, "Mesopause Dust as a Sink for Ionization," J. Geophys. Res., 81:2392.

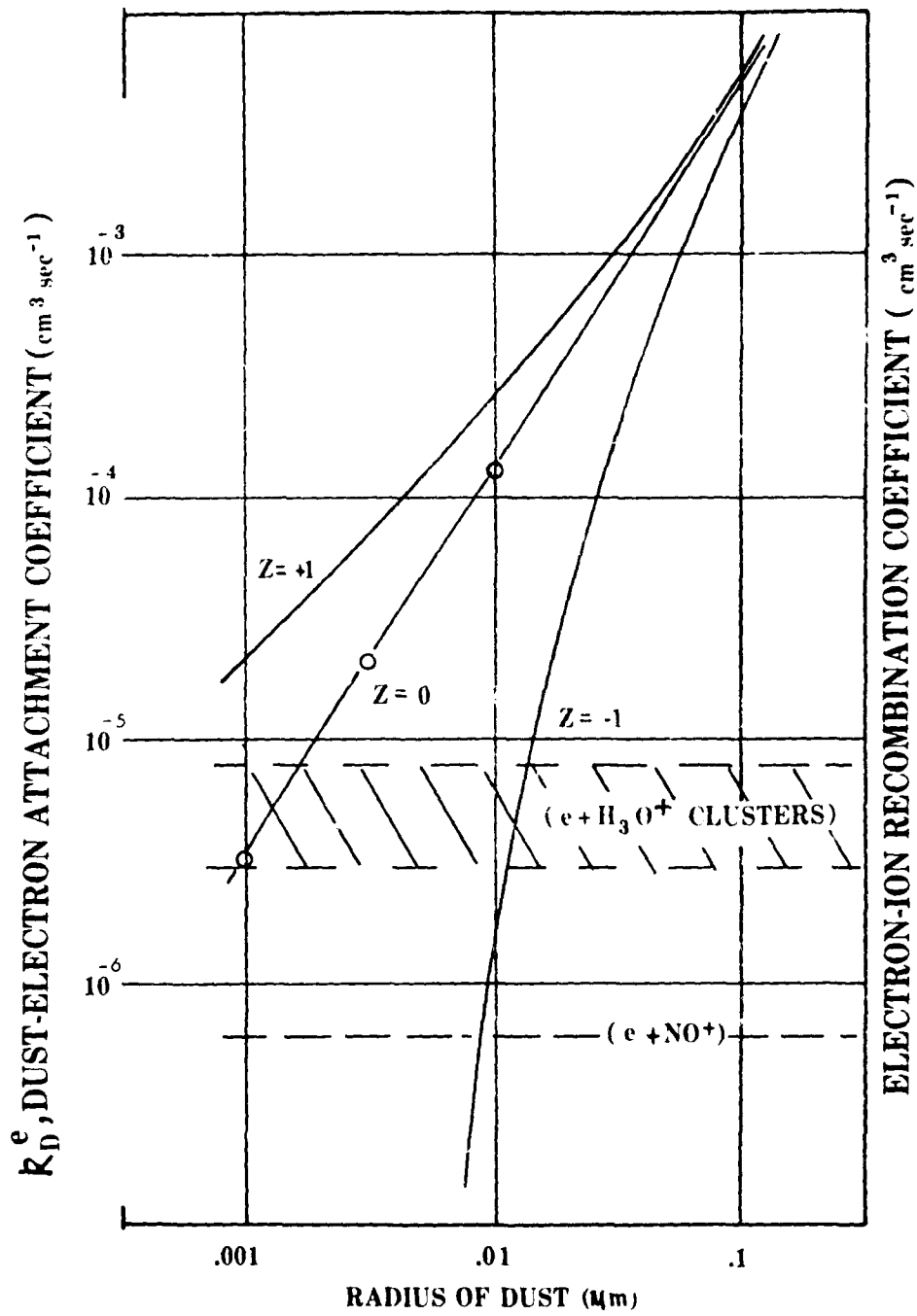


Figure 2. A plot showing the magnitude of  $k_D^e$ , the dust-electron attachment coefficient (left ordinate), for various radii of dust of charge  $Z = -1, 0, +1$ . For comparative purposes the electron-ion recombination coefficient for nitric oxide ions and water cluster ions is plotted on the right ordinate.

Expressed algebraically,

$$P_z (v_z^+ + v_z^e + v_z^- + v_{ph}) = P_{z+1} (v_{z+1}^e + v_{z+1}^-) + P_{z-1} (v_{z-1}^+ + v_{ph}) . \quad (3)$$

By setting  $P_z = 0$  for a large value of charge (say  $z = -9$ , meaning that no dust has 9 or more electrons on it), and solving the other  $P_z$ 's in terms of  $P_{-8}$  and so forth, a recursion relation may be obtained. Then, after normalizing with  $\sum P_z = 1$ , solve for each  $P_z$ . Neglecting negative ions for the daytime D region, the effective attachment coefficients are then defined as:

$$K_D^+ = \frac{1}{N_e} \sum P_z v_z^+ = \frac{1}{N_e} \sum P_z (v_z^e - v_{ph}) ; \quad (4)$$

$$K_D^+ = \frac{1}{N_e} \sum P_z v_z^e - \frac{\sum P_z v_{ph}}{N_e} . \quad (5)$$

The attachment coefficient for electrons,  $K_D^e$ , is:

$$K_D^e = \frac{\sum P_z v_z}{N_e} . \quad (6)$$

Substituting equation (6) into (5) and remembering  $\sum P_z = 1$ ,

$$K_D^+ = K_D^e - \frac{v_{ph}}{N_e} , \quad (7)$$

that is, the effective attachment coefficient for positive ions is equal to the effective attachment coefficient for electrons diminished by the photodetachment frequency divided by the ambient electron density.

This formulation incorporates the following assumptions and restrictions which limit its applicability to D region time dependent chemical codes:

- a. This formulation is explicitly stationary. An equilibrium is assumed between the rate of attachment and detachment of ions and electrons for the

derivation of the  $P_z$  fractions and the coefficients. As such, these coefficients are unsuitable for use in time dependent programs designed for rapidly varying atmospheric conditions such as eclipse times, sunrise and sunset, or nuclear burst phenomena.

b. It is assumed that  $N_e = \Sigma N_+$ . This assumption of charge neutrality among electrons and ions is equivalent to the assumption that the number of particulates is too small to perturb the charge balance, which may be an unrealistic assumption for the mesosphere. Therefore, since the derived  $P_z$  values are functions of the  $N_e$  or  $\Sigma N_+$  used, the calculation of new  $P_z$ 's and the effective coefficients would have to be handled iteratively in a computer code each time new  $N_e$  and  $\Sigma N_+$  were computed.

c. This formulation (equation 3) neglects competitive chemical attachment processes such as the recombination reactions between positive ions and electrons which would change  $P_z$  values and  $K_D^e$  and  $K_D^+$ .

Within these restrictions the values of  $K_D^e$  and  $K_D^+$  derived by Parthasarathy<sup>7</sup> are useful for steady state chemical codes with a comparatively small number of particulates. But if no restriction is to be placed upon the size of the dust population or upon the concentrations of electrons or positive ions, then a set of stepwise reactions utilizing the coefficients for individual dust in various charge states is more appropriate (section 2). However, a benefit of the approach by Parthasarathy is to predict the range and stability of resident charge loading expected on a population of dust under various ambient conditions. Thus, the number of piecewise reactions sufficient for dust of a given size may be predicted for use in the chemical reaction code.

#### 4.2 Choice of Photodetachment Coefficient for Dust

The photodetachment rate for the dust particle,  $\nu_{ph}$ , is a key and governing parameter in these computations. Photodetachment yields of many materials are difficult to measure in a laboratory, and, in turn, whether such measurements would be valid for mesospheric conditions is difficult to assess. The best that may be done is to assume a likely composition for dust and establish a plausible range for the photoelectric yield over the incident solar wavelengths which exist in the mesosphere.

Photoelectric yield of a given material is a function of many parameters such as surface roughness, angle of incidence of photons, temperature, and possible adsorption of gases on the surface. For example, photoelectric yield will

---

<sup>7</sup>R. Parthasarathy, 1976, "Mesopause Dust as a Sink for Ionization," J Geophys Res, 81:2392.

increase with greater roughness and angle of incidence.<sup>23</sup> Adsorption of gases such as molecular oxygen or hydrogen onto the surface may reduce the yield and shift the cutoff wavelength further into the ultraviolet;<sup>24</sup> whereas very small amounts of gases may increase yield and shift the cutoff wavelength to longer wavelengths through the formation of surface "double layers" which allow the creation of surface states about 0.4 ev below the Fermi level.<sup>25</sup>

If meteoritic material from galactic space, possibly ice coated, is assumed to be the constituent of the dust particles, then the photodetachment values for moon dust,<sup>26</sup> nickel,<sup>23</sup> or ice<sup>6</sup> would be reasonable options. Presumably, C-region meteoritic depositions would be of similar material to lunar surface dust. Willis et al.<sup>23</sup> determined the photoelectric yield of samples of moon dust from the Apollo 14 and 15 missions. Their determinations for moon dust were made at  $10^{-7}$  to  $10^{-9}$  torr, a more absolute vacuum than in the C-region by five orders of magnitude. Impurities in the samples were baked out for 1 hr. at 150°C. Auger electron spectroscopy and chemical analysis yielded a composition of: 48 percent of  $\text{SiO}_2$ , 18 percent of  $\text{Al}_2\text{O}_3$ , 11 percent of  $\text{CaO}$ , 10 percent of  $\text{FeO}$ , etc., which agrees with other determinations of composition for silicate-type meteors.<sup>26</sup> Peak emission of  $10^{11}$  electrons per photon occurs at 800 angstroms, with smaller values of  $10^{10}$  at 2500 angstroms and  $10^{7.5}$  at 600 angstroms. For solar flux at the top of the earth's atmosphere the composite yield is  $2.8 \times 10^9 (\pi a^2)$  photoelectrons per second for lunar surface material, where  $\pi a^2$  represents the surface area in square centimeters. Attenuation of solar flux in the Schumann-Runge Bands and Lyman  $\alpha$  in the mesosphere reduces this photodetachment frequency of neutral dust at 80 km to about  $1 \times 10^9 (\pi a^2) \text{ s}^{-1}$ . Since iron and nickel meteorites have been commonly reported,<sup>26</sup> the photoelectric yield for elemental nickel was obtained in Weissler.<sup>23</sup> When the appropriate solar flux is used for Lyman  $\alpha$  and the Schumann-Runge Bands attenuation at 80 km is accounted for, the resultant photodetachment for nickel is  $1.5 \times 10^9 (\pi a^2) \text{ s}^{-1}$ . Values of photodetachment for ice<sup>6</sup> are  $1.9 \times 10^8 (\pi a^2) \text{ s}^{-1}$ . To bracket these previous determinations for different materials and to allow for the considerable uncertainty which still remains, the following values of photodetachment frequency are chosen to

<sup>23</sup>G. L. Weissler, 1956, "Photoionization in Gases and Photoelectric Emission from Solids," in Handbuch der Physik, Vol XXI, Springer-Verlag, 304-382.

<sup>24</sup>B. Feuerbacher and B. Fitton, 1972, "Photoemission from Surface States on Tungsten," Phys Rev Letters, 29(12):786.

<sup>25</sup>R. F. Willis, M. Anderegg, B. Feuerbacher, and B. Fitton, "Photoemission and Secondary Electron Emission from Lunar Surface Material," in Photon and Particle Interactions with Surfaces in Space, Proceedings of the 6th ESTAB Symposium, Noordwijk, the Netherlands, 26-29 September 1972. R. J. L. Grand, Ed., D. Reidel Publishing Co., Dordrecht-Holland/Boston - USA.

<sup>26</sup>R. Parthasarathy and D. B. Rai, 1966, "Effect of Meteoric Dust on the Effective Recombination Coefficient in the Lower Ionosphere," Radio Sci. 1:1401.

<sup>26</sup>J. A. Jacobs, R. D. Russell, and J. T. Wilson, 1959, Physics and Geology, McGraw Hill, NY.

be incorporated into the calculations of this report (expressed for zero optical depth):  $2.8 \times 10^{10} (\pi a^2) s^{-1}$ ,  $2.8 \times 10^9 (\pi a^2) s^{-1}$ ,  $2.8 \times 10^8 (\pi a^2) s^{-1}$ , and 0.

Since mesospheric particles may possess a negative or positive charge, the question arises as to whether an electrostatic potential on a dust particle would modify the photodetachment yield from that dust. Manka<sup>27</sup> explored the result of having an electrostatic charge on the surface of dust and the resultant Coulomb retarding of the photoelectron current. He was specifically interested in dust on the lunar surface and showed, for example, that the current density of photoelectrons suffered a reduction of 26 percent in emitted electrons with a single positive charge. Our calculations are not adjusted for this small effect. In the case of a negative potential, the magnitude of the photoelectron current was not modified. That is, negatively charged dust will provide the same photoelectron current as neutral dust and obey the same wavelength dependence. Photoemission will not be enhanced.

A final comment is necessary about the differences in photoemission between single molecules and a solid composed of many molecules: It was considered possible that dust could photoemit in the visible, a fact suggested by analogy in the work of Woo et al<sup>28</sup> who described photoelectron detachment from the  $O_2^-$  molecule by visible wavelengths. This idea was supported by Chanin et al<sup>29</sup> who showed that electrons attaching to molecular oxygen to form  $O_2^-$  could possibly enter a  $v = 1$  vibrational state, described by a repulsive potential energy curve, which could then lead to autodetachment. However, in the case of a solid dust particle, such surface metastable states of high energy would not exist since the energy of the impacting electron would quickly dissipate as momentum and heat through neighboring atoms. The "extra" electron causing the unbalanced negative charge on a dust particle would be indistinguishable from any other electron occupying normal bound conduction states. Photoemission would always operate against the work function of the material and exhibit the same cutoff frequency for irradiation as that for an uncharged surface. Therefore, it would not be likely for dust to photoemit in the visible.

#### 4.3 Charge Loading on Dust

The first result of performing the calculation of the effective attachment coefficients,  $K_D^e$  and  $K_D^+$ , is the determination of the fractions of the dust

<sup>27</sup>R. H. Manka, "Plasma and Potential at the Lunar Surface," in Photon and Particle Interactions with Surfaces in Space, Proceedings of the 6th Eslab Symposium, Noordwijk, The Netherlands, 26-29 September 1972, D. Reidel Publishing Co., Dordrecht-Holland/Boston - USA.

<sup>28</sup>S. B. Woo, L. M. Branscomb, and E. C. Beaty, 1969, "Sunlight Photodetachment of Ground State  $O_2^-$ ," J Geophys Res, 74:2933.

<sup>29</sup>L. M. Chanin, A. V. Phelps, and M. A. Biondi, 1962, "Measurements of Attachment of Low Energy Electrons to Oxygen Molecules," Phys Rev, 128:219.

population which carry a particular charge. Table 2 lists the percentages of the total dust population which carry given numbers of electrons for dust of radii  $0.001\mu\text{m}$ ,  $0.01\mu\text{m}$ , and  $0.1\mu\text{m}$  under various ambient electron densities.

The tabulation reveals some of the most graphic aspects of dust behavior in the D region: For example, the charge for dust of radius  $0.01\mu\text{m}$ , or smaller, is one electron per dust particle. (These results are similar to those of figures 3 and 4 in Parthasarathy.) This loading holds for a wide range of ambient electron number densities of 100 to 10,000 centimeter $^{-3}$  and photodetachment values of 0 to  $10^7\text{ s}^{-1}$ . Under similar ambient conditions, dust sized midway between  $0.01\mu\text{m}$  to  $0.1\mu\text{m}$  holds a more or less stable charge of 2 to 3 electrons which shifts to 1 electron or no electrons at high photodetachment rates. Dust of radius  $0.1\mu\text{m}$  presents a less clean-cut picture. The normal loading is a broad distribution of 5, 6, or 7 electrons which is displaced to positive values of charge where photodetachment values  $>1\text{ s}^{-1}$  and electron densities below  $1000\text{ cm}^{-3}$  are used. In each of these cases, photodetachment does not exert an influence until it exceeds about  $1\text{ s}^{-1}$ .

This insensitivity to photodetachment rates below a certain threshold is an important result since a rigorous number for dust photodetachment rates has been hard to obtain, and this difficulty had been an area of uncertainty in chemical models. A further result is that the smaller dust sizes will exist in the D region with only a single negative charge if they are charged at all.

As an alternate way to illustrate the competing elements of this situation, figure 3 shows a plot of photodetachment frequency for moon dust and ice along with electron attachment frequency for dust charged  $Z = 1, 0, +1$  and frequency for the recombination of electrons with  $\text{N}_2^+$  and hydrated water cluster ions. An ambient electron and ion density of  $10^6\text{ cm}^{-3}$  has been used for this illustration.

From an examination of figure 3, a number of points are apparent:

a. Positively charged dust of any size can competitively acquire electrons when compared to normal electron-ion recombination processes. Uncharged dust of radius  $\gtrsim 0.002\mu\text{m}$  can compete effectively for electrons even when the positive ions are water clusters (as is the case for altitudes below 80 km). Negatively charged dust can only compete effectively for electrons if the particles have a radius  $\gtrsim 0.02\mu\text{m}$ . Dust with radii on the order of  $0.1\mu\text{m}$  could attach several electrons, but because of the nominally low number densities of  $0.1\mu\text{m}$  radius dust ( $\sim 10\text{ cm}^{-3}$ ), the overall electron attachment to dust of this size is probably of secondary importance when compared to the normal electron-ion recombination processes, a point already noted by Parthasarathy.<sup>7</sup> However, if dust particles of much smaller sizes were present in large numbers, as is most likely the case, then dust could appreciably alter the ambient electron and ion equilibrium densities. The precise effect

<sup>7</sup>R. Parthasarathy, 1976, "Mesopause Dust as a Sink for Ionization," J. Geophys. Res., 81:2392.

TABLE 2. PERCENT OF DUST POPULATION WITH A PARTICULAR NUMBER OF ELECTRONS FOR  $T = 150^\circ\text{K}^*$

Dust Particle Radius ( $\mu\text{m}$ )	Ambient Electron Density	Percentage								
		0.001			0.01			0.1		
		100	1000	10,000	100	1000	10,000	100	1000	10,000
Photodetachment	Charge (e)									
Rate ( $\text{s}^{-1}$ )	Z									
0	-4							7	6	6
	-5							28	28	28
	-6							40	40	40
	-7							20	20	20
	-8							3	3	3
$2.8 \times 10^8 (\pi a^2)$	0	2	2	2	1.3	0				
	-1	97	97	97	90	88	9			
	-2				8	11	30			
	-3						36	8		
	-4						17	28	9	
	-5						3	39	32	
	-6							20	39	
	-7							4	17	
	-8									3
$2.8 \times 10^9 (\pi a^2)$	0	22	5	2		0		2		
	-1	76	95	97		90		9		
	-2					8		30		
	-3						36	8		
	-4						18	28		
	-5						3	39		
	-6							20		
	-7							4		
$2.8 \times 10^{10} (\pi a^2)$	8							1		
	7							3		
	6							6		
	5							10		
	4							15		
	3							19		
	2	3					0		18	
	1	19					0		14	
	0	56	22	5			7			
	-1	20	76	95			90		6	1
	-2						2		3	9
	-3								1	30
	-4									36
	-5									17
										3

\*Columns may not always total 100 due to rounding and to neglecting states with less than 0.5 percent.

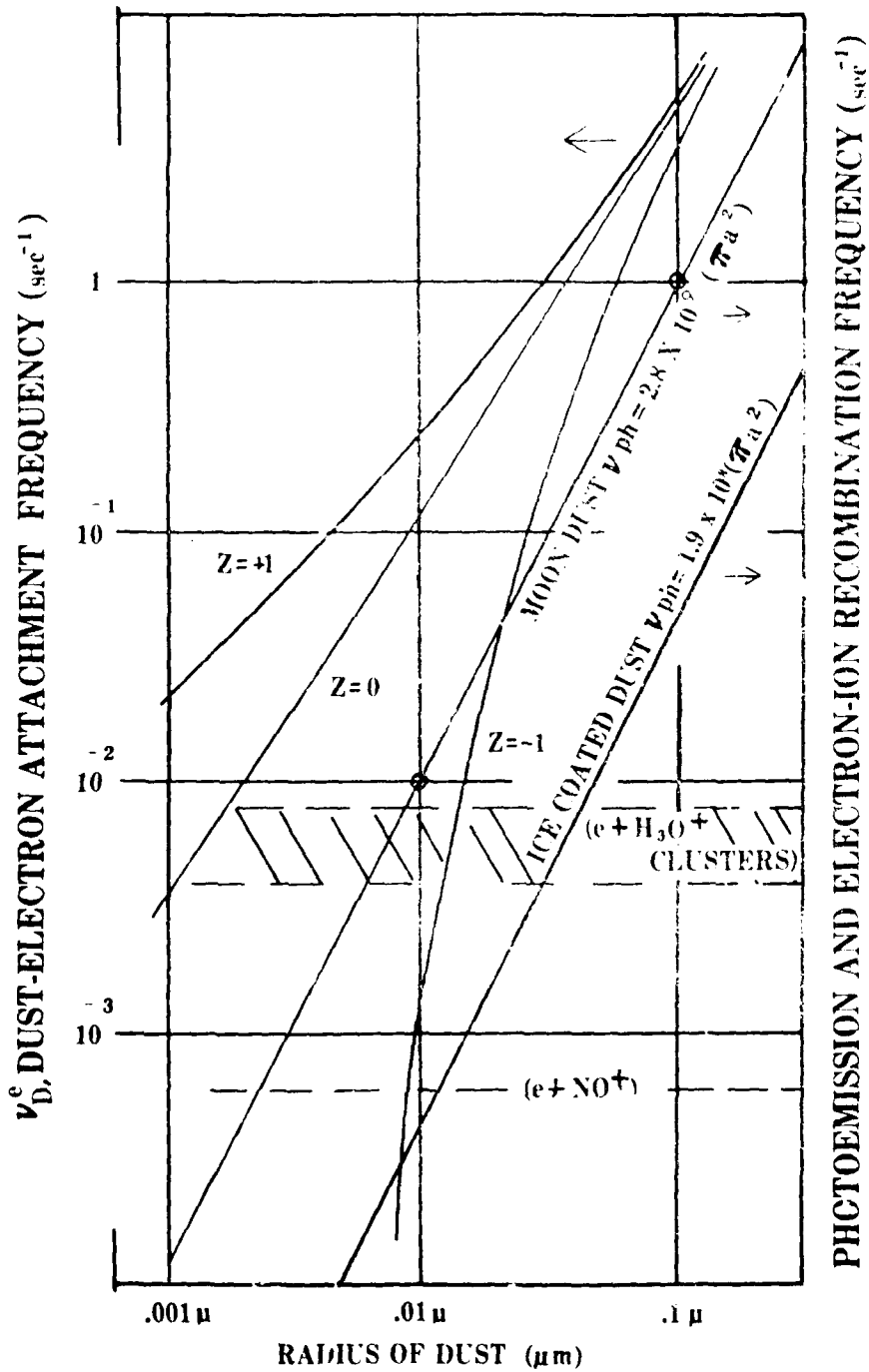


Figure 3. A plot showing the magnitude of  $\nu_D^e$ , the dust-electron attachment frequency (left ordinate) for various radii of dust of charge  $Z = -1, 0, +1$ . The electron-cluster ion and electron-nitric oxide ion recombination frequency is plotted on the right ordinate. An electron density of  $10^1 \text{ cm}^{-3}$  is assumed. Values of photoemission frequencies for various radii of moon dust and ice-coated moon dust are represented on the right ordinate.

EFFECTIVE ATTACHMENT COEFFICIENT,  $K_D^e$  &  $K_D^+$   
FOR DUST OF RADIUS .001  $\mu\text{m}$

EFFECTIVE ATTACHMENT COEFFICIENT,  $K_D^e$  &  $K_D^+$   
FOR DUST OF RADIUS .01  $\mu\text{m}$

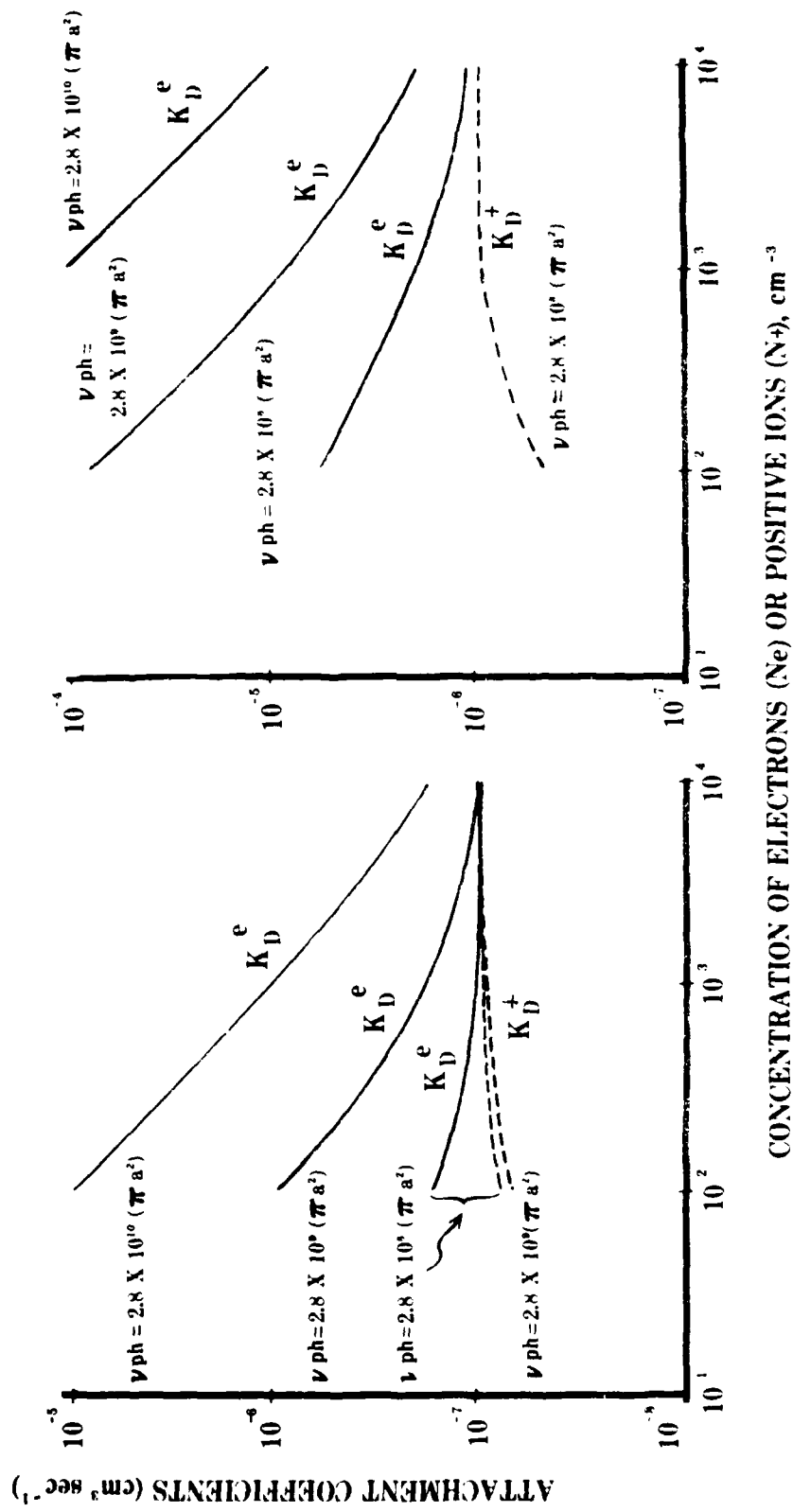


Figure 4. Values of the effective attachment coefficients of  $0.001 \mu\text{m}$  and  $0.01 \mu\text{m}$  dust to electrons,  $K_D^e$ , and positive ions,  $K_D^+$ , for populations of electrons and ions ranging from  $10$  to  $10^4 \text{ cm}^{-3}$ .

would depend on the rate of photoemission of the electrons from the negatively charged dust.

b. During twilight or nighttime, smaller particulates (radius  $< 0.01\mu\text{m}$ ) become negatively charged. Hence, in large numbers, small dust particles could compete effectively with ion-electron recombination and provide a means of maintaining (rather than neutralizing) negative charge. Referring to the right side of equation (6), the  $v_e^e$  term will dominate the tendency to lead all particles negatively; the photoemission term,  $v_{ph}$ , will tend to counter this. If  $v_{ph}$  is sufficiently large, keep the smaller particles neutral or even make them positive. At night, or for regions of low light levels, the  $v_{ph}^+$  term will dominate and drive a large fraction of the particulates positive.

c. Dust which is ice coated photoemits an order of magnitude less  $v_e^e$  than uncoated dust. This difference would mean that during polar night conditions with noctilucent clouds, a larger number of electrons could be attached to the ice coated dust than at other times of the year, resulting in a sharper reduction in the free electron density.

#### 4.4 Effective Dust Attachment Coefficients

Figure 4 shows one instructive example of the derived  $K_D^e$  and  $K_D^+$  values for 0.001 $\mu\text{m}$  and 0.01 $\mu\text{m}$  size dust plotted against electron density ( $N_e$ ) and three photodetachment values. The abscissa for figure 4 is  $N_e$  (or  $N_+$  since, by the requirement of charge neutrality, they must be held equal in the calculations). Immediately apparent from this graph is the great variability of  $K_D^e$  and  $K_D^+$  with changing electron and positive ion densities and photodetachment. Specifically: (a)  $K_D^e$  exceed  $K_D^+$  since electrons move 300 times as fast as positive ions and hence have a higher collisional frequency. (b) Higher values of photodetachment rates,  $v_{ph}$ , result in higher  $K_D^e$  values since photodetachment tends to keep a particle uncharged (or positively charged), which means that impacting electrons will not feel a repulsive force. (c) As the numbers of ambient electrons and ions increase, the  $K_D^e$  and  $K_D^+$  values converge to a common asymptote because the extreme ambient densities negate the effects of photodetachment. However, the fact that  $K_D^e$  and  $K_D^+$  are so highly dependent upon ambient electron and ion densities requires that they be entered iteratively into computer codes, a less efficient procedure than using a set of  $k_D^e$  and  $k_D^+$  for the individual charging reactions for dust.

## 5. THE EFFECTS OF DUST ON D REGION CHEMISTRY AND CHARGE BALANCE THROUGH THE USE OF A FULL CHEMICAL CODE

### 5.1 Runs at 80 km with Variable Dust Concentration and Photodetachment Frequencies

The results of the previous sections have been organized as piecewise calculations designed to gain insight into the behavior of dust in the mesosphere. In this final section, dust is entered as a full partner into an electron-ion reaction set to quantify the effects on the charge balance. The treatment of this topic is not exhaustive, but it is included in this report to establish the qualitative nature of the effect of dust in the D region. The chemistry reaction set is that of DAIRCHEM,<sup>10</sup> and the dust attachment coefficients used are  $k_d^e = 1.2 (-4) \text{ cm}^3 \text{ s}^{-1}$  for  $0.01\mu\text{m}$  dust (table 1). Dust is entered in several concentrations: 0, 100, 1000, and  $10,000 \text{ cm}^{-3}$ , and the resulting values in electron density,  $\text{NO}^+$ , and the sum of the hydrated water cluster ions are listed in table 3, examples 1 through 4. In these examples the photodetachment value is held at the value derived from Willis et al,<sup>25</sup>  $2.8 \times 10^9 (-a^2) \text{ s}^{-1}$ , and the dust concentration is varied by 4 orders of magnitude. A second set of examples, 5 through 7, tests the results using photodetachment rates which vary from 0.01 to 100 times the above value.

Examples 1 through 4 show that as the dust population increases from 0 to  $1000 \text{ cm}^{-3}$  and  $10,000 \text{ cm}^{-3}$ , the electron density decreases from a high of 453 to 191 and  $54 \text{ cm}^{-3}$ , respectively. Sixty-four percent of dust remains uncharged at high concentrations ( $10,000 \text{ cm}^{-3}$ ), and 28 percent is negatively charged. Besides the effect of reducing the electron density, another major change is the marked increase in water cluster ion population. This increase is due to the removal of electrons which would recombine with the cluster ions directly (that is, due to the lower ion-dust recombination rate). Total charge neutrality is maintained in the chemistry of these runs, although only a small subset of positive ion species entered in DAIRCHEM is listed in this table. (For example, nitric oxide clusters and other minor positive ion species are omitted.)

Examples 5 through 7 show that the variation in photodetachment is significant in modifying the free electron density. High photodetachment rates drive the dust more positive and hence release electrons. For an increase in photodetachment of 4 orders of magnitude, the free electrons increase from 118 to  $749 \text{ cm}^{-3}$ . For the most probable value of photodetachment (Willis' value of  $2.8 \times 10^9 (-a^2 \text{ cm}^2 \text{ s}^{-1})^{25}$ ), the electron density increases more than 60 percent over its value with no photodetachment.

<sup>10</sup>D. W. Hoock and M. G. Heaps, 1978, DAIRCHEM: A Computer Code to Model Ionization-Deionization Processes and Chemistry in the Middle Atmosphere. Users Manual, US Army Atmospheric Sciences Laboratory, White Sands Missile Range, NM.

<sup>25</sup>R. F. Willis, M. Anderegg, B. Feuerbacher, and B. Fitton, "Photoemission and Secondary Electron Emission from Lunar Surface Material," in Photon and Particle Interactions with Surfaces in Space, Proceedings of the 6th Estab Symposium, Noordwijk, The Netherlands, 26-29 September 1972. R. J. L. Grand, Ed., D. Reidel Publishing Co., Dordrecht-Holland/Boston - USA.

TABLE 3. VARIATION IN ELECTRON DENSITY AT 80 km DUE TO VARIABLE DUST CONCENTRATION AND PHOTODETACHMENT. RADIUS = 0.01  $\mu$ m. DAIRCHEM COMPUTER MODEL MIDLATITUDE CASE.  $v_{ph}$  IS LISTED FOR ZERO OPTICAL DEPTH AND AN UNCHARGED PARTICLE.

Photodetachment, $v_{ph}$	Example	Dust Entered	Uncharged		Dust(+)	Dust(-)	Electron Density	$NO^+$ Ion Density	Sum Water Cluster Ions
			Dust	Dust					
$2.8 \times 10^9 (\pi a^2)$	1	0	0	0	0	0	453	102	207
	2	100	23	1	76	406	103	232	
	3	1000	384	13	603	191	111	507	
	4	10000	6423	759	2818	54	117	1818	
$2.8 \times 10^{10} (\pi a^2)$	5	1000	11	$10^{-3}$	989	118	114	823	
	6	1000	384	13	603	141	111	507	
	7	1000	524	443	33	749	94	118	

In each set of test runs the  $\text{NO}^+$  population is comparatively stable. In addition to the reactions listed below, a set of attachment reactions of positive ions to neutral, negatively charged, and positively charged dust was also used.



### 5.2 Comparison of the Effect of Four Dust Profiles ( $r = 0.01\mu\text{m}$ and $r = 0.001\mu\text{m}$ ) upon D-region Ion Chemistry.

As a more graphic test of the possibility of dust modifying the electron profiles of the D region, four dust distributions were included in the DAIRCHEM code, and computations were made at a series of altitudes. As a basis of comparison for the modeling, a standard type of observed electron density profile from daytime,  $\chi = 60^\circ$  at Wallops Island, VA, in December is presented. Secondly, the electron density profile computed by DAIRCHEM with no dust included is plotted. The other curves are computed electron densities using  $0.01\mu\text{m}$  dust at constant concentrations of 100 and  $1000 \text{ cm}^{-3}$  and  $0.001\mu\text{m}$  dust at concentrations of 1000 and  $5000 \text{ cm}^{-3}$ . These values bracket the estimates generally accepted for dust concentrations in that region. The values are tabulated in table 4. A photodetachment value of  $2.8 \times 10^9 (\pi a^2) \text{ s}^{-1}$  was used for dust for all runs.

TABLE 4. SELECTED DUST PROFILES

Altitude (km)	A	No Dust	B $0.01\mu\text{m}$	C	D $0.001\mu\text{m}$	E
100	0	100	1000	1000		
90	0	100	1000	1000	5000	
85	0	100	1000	1000		
80	0	100	1000	1000	5000	
75	0	100	1000	1000		
70	0	100	1000	1000	5000	
60	0	100	1000	1000		

The dust profiles used as input to the code represent a plausible range of values. However, since the distribution of dust in the upper mesosphere is a very open question, these profiles were felt to be adequate in a preliminary demonstration of the DAIRCHEM results to dust, particularly the charge

balance. A "step" profile of dust (i.e., a sharp ledge of dust at a given altitude) has been conjectured in the literature. This effect may easily be seen by the comparison, at any altitude, of the dust case with the no dust case.

The results of these inputs to DAIRCHEM are plotted in figure 5. Curve 1 is the Wallops Island observation of electron density for December with  $\chi = 60^\circ$ . This profile shows the abrupt change in slope at 82 km that is commonly observed in many electron density profiles in the D region under quiet conditions. Curve 2 is the computed electron density profile using DAIRCHEM with no dust. Note the divergence of these two curves at 87 to 75 km. Curves 3 and 4 are  $0.01\mu\text{m}$  dust at concentrations of  $100 \text{ cm}^{-3}$  and  $1000 \text{ cm}^{-3}$ . A reduction in electron concentration is apparent at 85 to 78 km, particularly for the  $1000 \text{ cm}^{-3}$  distribution. Below 78 km, the reduction in electron density exceeds the observed curve 1, possibly suggesting that dust may be confined in a relatively narrow ledge. For example, the best fit using  $0.01\mu\text{m}$  dust would be in excess of  $1000 \text{ cm}^{-3}$  from 85 to 77 km and dropping to about  $200 \text{ cm}^{-3}$  by 70 km. Curves 5 and 6,  $0.001\mu\text{m}$  dust at  $1000$  and  $5000 \text{ cm}^{-3}$ , bracket the observed values of electron density down to 77 km. Optimum concentration for  $0.001\mu\text{m}$  dust would be  $3000$  to  $4000 \text{ cm}^{-3}$ . Below 77 km the reducing action of this dust is clearly excessive, thus suggesting values near  $200 \text{ cm}^{-3}$  at 70 km.

Although these calculations were run at each 5 km in altitude and with a limited number of cases, the results clearly show that a judicious choice of dust concentration can allow the modeled electron density to reproduce the heretofore "anomalous bite-outs" in electron density often observed around 80 km. The controlling rule is: if the particle concentration equals or exceeds the model electron density computed by vapor phase reactions alone, such as in the case below 85 km, a reduction to observed values is apparent. Most runs of DAIRCHEM indicate the best fit is with a variable concentration of dust with altitude.

## 6. SUMMARY AND CONCLUSIONS

The purpose of this report has been to examine, through a series of piecewise calculations and comparisons, the importance of electron-dust attachment to D region chemistry, particularly in competition with electron-ion recombination. In the course of the argument, we have examined the preferred charge loadings on a population of dust and generated two different (but related) sets of coefficients for electron or positive ion dust attachment calculations. The discrete attachment coefficients,  $k_D^e$  and  $k_D^+$ , should generally be used in chemical computer codes since they result in knowledge of the precise charge loading of individual dust particles.

Dust of radius less than  $0.01\mu\text{m}$  acquires only one electron under mesospheric conditions. Dust of radius  $0.1\mu\text{m}$  may acquire as many as five or six resident electrons, and in this size range photodetachment does not perturb the distribution of charge loading too greatly. The size of dust therefore seems to predetermine a unique charge loading for each dust particle over a wide range of photodetachment values. An accurate measurement of dust size and

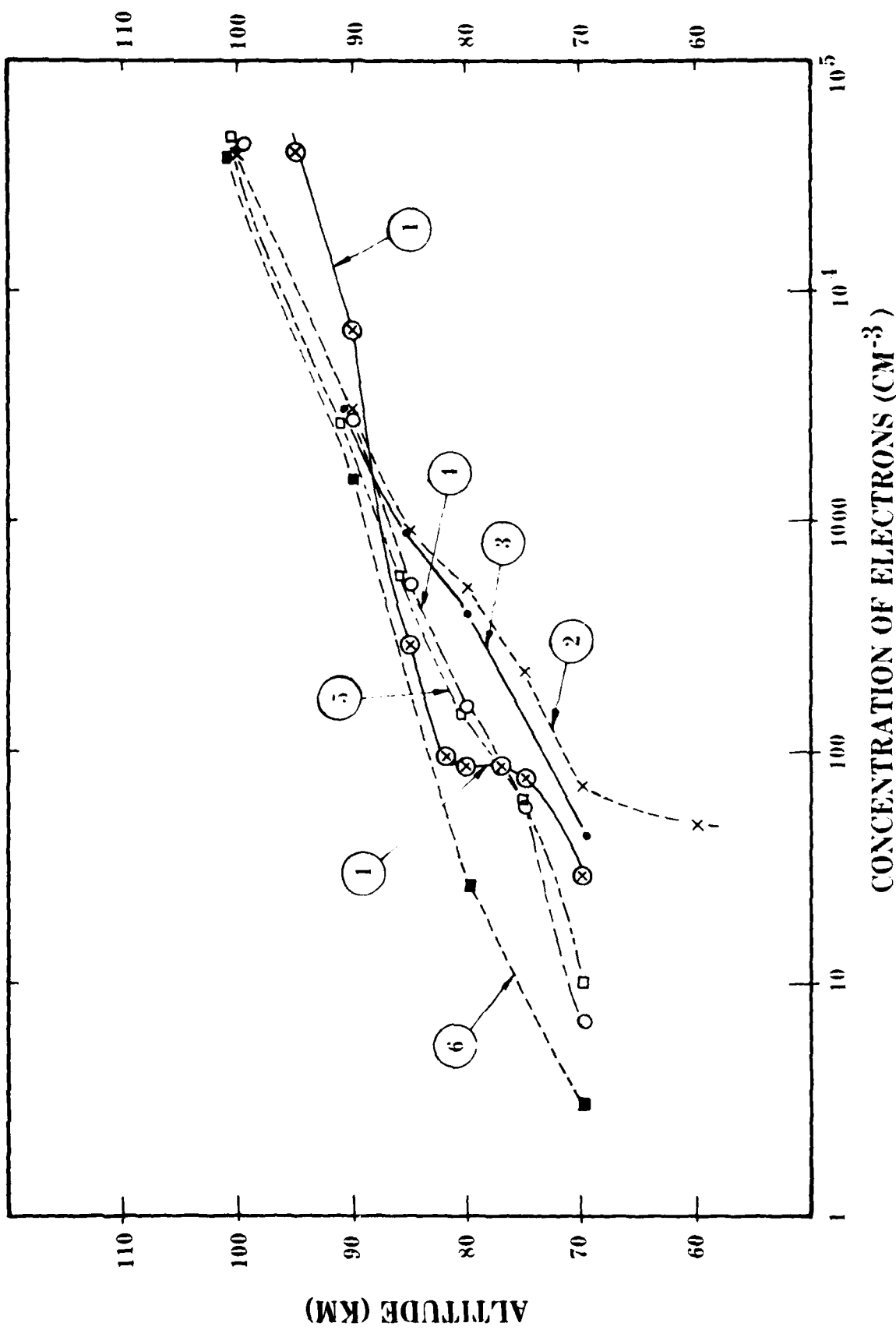


Figure 5. A plot of observed electron densities at Wallops Island, VA, for December (curve 1), model computation by DAIRCHEM from the case of no dust (curve 2), 0.01 $\mu$ m dust concentrations of 100  $\text{cm}^{-3}$ , and 1000  $\text{cm}^{-3}$ , at all altitudes (curves 3 and 4), and 0.001 $\mu$ m dust at concentrations of 1000  $\text{cm}^{-3}$ , and 5000  $\text{cm}^{-3}$ , (curves 5 and 6).

concentration could permit one to reasonably estimate its effect upon the chemistry due to this unique property. The full understanding of the role of dust, however, requires the use of the ion kinetic reaction scheme.

This report ameliorates some uncertainty in photodetachment rates by running a set of calculations of DAIRCHEM using  $v_{ph}$  orders of magnitude lower and higher than the value used by previous researchers and showing resultant stability in the computed electron densities. Nevertheless, the previous value, obtained from moon dust, seems to be the most logical for use in further D region chemistry runs. Based upon the limited computations made for this study, dust indeed does appear to compete strongly for electrons, particularly at dust concentrations of around  $1000 \text{ cm}^{-3}$ .

Figure 5 represents the most advanced set of calculations of this report and demonstrates that it is possible, with a proper choice of a dust profile and size, to approximate several heretofore "anomalous features" in electron density profiles.

The concentrations of dust included here for use at 80 km were consistent with reports from the literature. The next step in pursuing this topic must be the analytic derivation of a dust size concentration profile starting, most logically, with meteor flux estimates at 150 km. This present model has been run strictly for daytime chemistry and has purposely neglected nighttime processes and the attachment of negative ions to dust at night. Until this other important step is taken and an extensive series of runs is made, a description of the role of dust in D region chemistry will remain incomplete.

## REFERENCES

1. Hunten, D. M., R. P. Turco, and O. B. Toon, 1980, "Smoke and Dust Particles of Meteoric Origin in the Mesosphere and Stratosphere," J Atmos Sci, 37:1342.
2. Pedersen, A., J. Troin, and J. A. Kane, 1979, "Rocket Measurements Showing a Removal of Electrons Above the Mesopause in Summer at High Latitude," Planet Space Sci, 18:945-947.
3. Heaps, M. G., F. E. Niles, and R. D. Sears, 1978, Modeling the Ion Chemistry of the D-region: A Case Study Based Upon the 1966 Total Solar Eclipse, ASL-TR-0015, US Army Atmospheric Sciences Laboratory, White Sands Missile Range, NM.
4. Heaps, M. G., and J. M. Heimer', 1980, "The Quiet Midlatitude D-region: A Comparison Between Modeling Efforts and Experimental Efforts," J Atmos Terr Phys, 42:733.
5. Mechtly, E. A., C. F. Sechrist, Jr., and L. G. Smith, 1972, "Electron Loss Coefficients for the D-region and the Ionosphere from Rocket Measurements During the Eclipses of March 1970 and November 1966," J Atmos Terr Phys, 34:641.
6. Parthasarathy, R., and D. B. Rai, 1966, "Effect of Meteoric Dust on the Effective Recombination Coefficient in the Lower Ionosphere," Radio Sci, 1:1401.
7. Parthasarathy, R., 1976, "Mesopause Dust as a Sink for Ionization," J Geophys Res, 81:2392.
8. Hamilton, R. A., 1964, "Observations of Noctilucent Clouds Near Midwinter," Met Mag Lond, 93:201.
9. Donahue, T. M., B. Guenther, and J. E. Blamont, 1972, "Noctilucent Clouds in the Daytime: Circumpolar Particulate Layers Near the Summer Mesopause," J Atmos Sci, 29(6):1205.
10. Witt, G., 1960, "Polarization of Light from Noctilucent Clouds," J Geophys Res, 65:925-933.
11. Fogle, B., and M. Rees, 1972, "Spectral Measurements of Noctilucent Clouds," J Geophys Res, 77:720.
12. Divari, G., 1964, "The Dust Concentration in the Upper Layers of the Earth's Atmosphere," Geomagnetism and Aeronomy, 4:688-692.
13. Hunten, D. M., 1975, Vertical Transport in Atmospheres, Atmospheres of Earth and the Planets, D. Reidel Publishing Co., Dordrecht-Holland, pp 57-72.
14. Witt, G., 1969, "The Nature of Noctilucent Clouds," Space Res, IX:157-169, North Holland Publishing Co.

15. Narcisi, R. D., and A. D. Bailey, 1965, "Mass Spectrometric Measurements of Positive Ions at Altitudes from 64 to 112 Kilometers," J Geophys Res., 70:3687.
16. Arnold, F., and W. Joos, 1979, "Rapid Growth of Atmospheric Cluster Ions at the Cold Mesopause," Geophys Res Letters, 6:763-766.
17. Castleman, A. W., Jr., 1974, "Nucleation Processes and Aerosol Chemistry," Space Sci Rev, 15:547-589.
18. Castleman, A. W., Jr., 1979, "Nucleation and Molecular Clustering of Ions," Adv in Colloid and Interface Sci, 10:73-128.
19. Reid, G. C., 1975, "Ice Clouds at the Summer Polar Mesopause," J Atmos Sci, 32:523.
20. Chapman, S., and P. C. Kendall, 1965, "Noctilucent Clouds and Thermospheric Dust: Their Diffusion and Height Distribution," Quart J Roy Met Soc, 91:115.
21. Clemesha, B. R., V. W. J. H. Kirchoff, D. M. Simonich, and H. Takahashi, 1978, "Evidence of an Extra-Terrestrial Source for the Mesospheric Sodium Layer," Geophys Res Letters, 5:873-877.
22. Natanson, G. L., 1960, "On the Theory of the Charging of Amicroscopic Aerosol Particles as a Result of the Capture of Gas Ions," Sov Phys Tech Phys, (English Translation), 5:538.
23. Weissler, G. L., 1956, "Photoionization in Gases and Photoelectric Emission from Solids," in Handbuch der Physik, Vol XXI, Springer-Verlag, 304-382.
24. Feuerbacher, B., and B. Fitton, 1972, "Photoemission from Surface States on Tungsten," Phys Rev Letters, 29(12):786.
25. Willis, R. F., M. Anderegg, B. Feuerbacher, and B. Fitton, "Photoemission and Secondary Electron Emission from Lunar Surface Material," in Photon and Particle Interactions with Surfaces in Space, Proceedings of the 6th Eslab Symposium, Noordwijk, The Netherlands, 26-29 September 1972, R. J. L. Grand, Ed., D. Reidel Publishing Co., Dordrecht-Holland/Boston - USA.
26. Jacobs, J. A., R. D. Russell, and J. T. Wilson, 1959, Physics and Geology, McGraw Hill, NY.
27. Manka, R. H., "Plasma and Potential at the Lunar Surface," in Photon and Particle Interactions with Surfaces in Space, Proceedings of the 6th Eslab Symposium, Noordwijk, The Netherlands, 26-29 September 1972, D. Reidel Publishing Co., Dordrecht-Holland/Boston - USA.
28. Woo, S. B., L. M. Branscomb, and E. C. Beatty, 1969, "Sunlight Photodetachment of Ground State O<sub>2</sub>," J Geophys Res, 74:2933.

29. Chanin, L. M., A. V. Phelps, and M. A. Biondi, 1962, "Measurements of Attachment of Low Energy Electrons to Oxygen Molecules," Phys Rev, 128:219.

30. Hoock, D. W., and M. G. Heaps, 1978, DAIRCHEM: A Computer Code to Model Ionization-Deionization Processes and Chemistry in the Middle Atmosphere. Users Manual, March 1978, US Army Atmospheric Sciences Laboratory, White Sands Missile Range, NM.

ELECTRO-OPTICS DISTRIBUTION LIST

Commander  
US Army Aviation School  
Fort Rucker, AL 36362

Commander  
US Army Aviation Center  
ATTN: ATZQ-D-MA (Mr. Oliver N. Heath)  
Fort Rucker, AL 36362

Commander  
US Army Aviation Center  
ATTN: ATZQ-D-MS (Mr. Donald Wagner)  
Fort Rucker, AL 36362

NASA/Marshall Space Flight Center  
ATTN: ES-83 (Otha H. Vaughan, Jr.)  
Huntsville, AL 35812

NASA/Marshall Space Flight Center  
Atmospheric Sciences Division  
ATTN: Code ES-81 (Dr. William W. Vaughan)  
Huntsville, AL 35812

Nichols Research Corporation  
ATTN: Dr. Larry W. Pinkley  
4040 South Memorial Parkway  
Huntsville, AL 35802

John M. Hobbie  
c/o Kentron International  
2003 Byrd Spring Road  
Huntsville, AL 35802

Mr. Ray Baker  
Lockheed-Missile & Space Company  
4800 Bradford Blvd  
Huntsville, AL 35807

Commander  
US Army Missile Command  
ATTN: DRSMI-OG (Mr. Donald R. Peterson)  
Redstone Arsenal, AL 35809

Commander  
US Army Missile Command  
ATTN: DRSMI-OGA (Dr. Bruce W. Fowler)  
Redstone Arsenal, AL 35809

Commander  
US Army Missile Command  
ATTN: DRSMI-REL (Dr. George Emmons)  
Redstone Arsenal, AL 35809

Commander  
US Army Missile Command  
ATTN: DRSMI-REO (Huey F. Anderson)  
Redstone Arsenal, AL 35809

Commander  
US Army Missile Command  
ATTN: DRSMI-REO (Mr. Maxwell W. Harper)  
Redstone Arsenal, AL 35809

Commander  
US Army Missile Command  
ATTN: DRSMI-REO (Mr. Gene Widenhofer)  
Redstone Arsenal, AL 35809

Commander  
US Army Missile Command  
ATTN: DRSMI-RHC (Dr. Julius Q. Lilly)  
Redstone Arsenal, AL 35809

Commander  
US Army Missile Command  
Redstone Scientific Information Center  
ATTN: DRSMI-RPRD (Documents Section)  
Redstone Arsenal, AL 35809

Commander  
US Army Missile Command  
ATTN: DRSMI-RRA (Dr. Oskar Essenwanger)  
Redstone Arsenal, AL 35809

Commander  
US Army Missile Command  
ATTN: DRSMI-RR0 (Mr. Charles Christensen)  
Redstone Arsenal, AL 35809

Commander  
US Army Missile Command  
ATTN: DRSMI-RR0 (Dr. George A. Tanton)  
Redstone Arsenal, AL 35809

**Commander**  
US Army Communications Command  
ATTN: CC-OPS-PP  
Fort Huachuca, AZ 85613

**Commander**  
US Army Intelligence Center & School  
ATTN: ATSI-CD-CS (Mr. Richard G. Cundy)  
Fort Huachuca, AZ 85613

**Commander**  
US Army Intelligence Center & School  
ATTN: ATSI-CD-MD (Mr. Harry Wilder)  
Fort Huachuca, AZ 85613

**Commander**  
US Army Intelligence Center & School  
ATTN: ATSI-CS-C (2LT Coffman)  
Fort Huachuca, AZ 85613

**Commander**  
US Army Yuma Proving Ground  
ATTN: STEYP-MSA-TL  
Bldg 2105  
Yuma, AZ 85364

**Northrop Corporation**  
Electro-Mechanical Division  
ATTN: Dr. Richard D. Tooley  
500 East Orangethorpe Avenue  
Anaheim, CA 92801

**Commander**  
Naval Weapons Center  
ATTN: Code 3918 (Dr. Alexis Shlanta)  
China Lake, CA 93555

**Hughes Helicopters**  
Army Advanced Attack Helicopter Weapons  
ATTN: Mr. Charles R. Hill  
Centinela and Teale Streets  
Bldg 305, MS T-73A  
Culter City, CA 90230

**Commander**  
US Army Combat Developments  
Experimentation Command  
ATTN: ATEC-PL-M (Mr. Gary G. Love)  
Fort Ord, CA 93941

**SRI International**  
ATTN: K2060/Dr. Edward E. Utthe  
333 Ravenswood Avenue  
Menlo Park, CA 94025

**SRI International**  
ATTN: Mr. J. E. Van der Laan  
333 Ravenswood Avenue  
Menlo Park, CA 94025

**Jane May**  
Nav. Environmental Prediction  
Research Facility (NEPRF)  
ATTN: Library  
Monterey, CA 93940

**Sylvania Systems Group,**  
Western Division  
GTE Products Corporation  
ATTN: Technical Reports Library  
P.O. Box 205  
Mountain View, CA 94042

**Sylvania Systems Group**  
Western Division  
GTE Products Corporation  
ATTN: Mr. Lee W. Carrier  
P.O. Box 188  
Mountain View, CA 94042

**Pacific Missile Test Center**  
Geophysics Division  
ATTN: Code 3250-3 (R. de Violini)  
Point Mugu, CA 93042

**Pacific Missile Test Center**  
Geophysics Division  
ATTN: Code 3253 (Terry E. Battalino)  
Point Mugu, CA 93042

**Effects Technology Inc.**  
ATTN: Mr. John D. Carlyle  
5383 Hollister Avenue  
Santa Barbara, CA 93111

**Commander**  
Naval Ocean Systems Center  
ATTN: Code 532 (Dr. Juergen Richter)  
San Diego, CA 92152

**Commander**  
Naval Ocean Systems Center  
ATTN: Code 5322 (Mr. Herbert G. Hughes)  
San Diego, CA 92152

**Commander**  
Naval Ocean Systems Center  
ATTN: Code 4473 (Tech Library)  
San Diego, CA 92152

**The RAND Corporation**  
ATTN: Ralph Huschke  
1700 Main Street  
Santa Monica, CA 90406

**Particle Measuring Systems, Inc.**  
ATTN: Dr. Robert G. Knollenberg  
1855 South 57th Court  
Boulder, CO 80301

**US Department of Commerce**  
National Oceanic and Atmospheric Admin  
Environmental Research Laboratories  
ATTN: Library, R-51, Technical Reports  
325 Broadway  
Boulder, CO 80303

**US Department of Commerce**  
National Oceanic and Atmospheric Admin  
Environmental Research Laboratories  
ATTN: R45X3 (Dr. Vernon E. Derr)  
Boulder, CO 80303

**US Department of Commerce**  
National Telecommunications and  
Information Administration  
Institute for Telecommunication Sciences  
ATTN: Code 1-3426 (Dr. Hans J. Liebele)  
Boulder, CO 80303

**AFATL/DLOOL**  
Technical Library  
Eglin AFB, FL 32542

**Commanding Officer**  
Naval Training Equipment Center  
ATTN: Technical Information Center  
Orlando, FL 32813

**Georgia Institute of Technology**  
Engineering Experiment Station  
ATTN: Dr. Robert W. McMillan  
Atlanta, GA 30332

**Georgia Institute of Technology**  
Engineering Experiment Station  
ATTN: Dr. James C. Wiltse  
Atlanta, GA 30332

**Commandant**  
US Army Infantry Center  
ATTN: ATSH-CD-MS-E (Mr. Robert McKenna)  
Fort Benning, GA 31805

**Commander**  
US Army Signal Center & Fort Gordon  
ATTN: ATZHCD-CS  
Fort Gordon, GA 30905

**Commander**  
US Army Signal Center & Fort Gordon  
ATTN: ATZHCD-O  
Fort Gordon, GA 30905

**USAFAF/AF-101**  
ATTN: Mr. Charles Glauber  
Scott AFB, IL 62225

**Commander**  
Air Weather Service  
ATTN: AWS/DNDP (LTC Kit G. Cottrell)  
Scott AFB, IL 62225

**Commander**  
Air Weather Service  
ATTN: AWS/DODF (MAJ Robert Wright)  
Scott AFB, IL 62225

**Commander**  
US Army Combined Arms Center  
& Ft. Leavenworth  
ATTN: ATZLCA-CAA-Q (Mr. H. Kent Pickett)  
Fort Leavenworth, KS 66027

**Commander**  
US Army Combined Arms Center  
& Ft. Leavenworth  
ATTN: ATZLCA-SAN (Robert Dekinder, Jr.)  
Fort Leavenworth, KS 66027

**Commander**  
US Army Combined Arms Center  
& Ft. Leavenworth  
ATTN: ATZLCA-SAN (Mr. Kent I. Johnson)  
Fort Leavenworth, KS 66027

**Commander**  
US Army Combined Arms Center  
& Ft. Leavenworth  
ATTN: ATZLCA-WE (LTC Darrell Holland)  
Fort Leavenworth, KS 66027

**President**  
USAARENBD  
ATTN: ATZK-AE-TA (Dr. Charles R. Leake)  
Fort Knox, KY 40121

**Commander**  
US Army Armor Center and Fort Knox  
ATTN: ATZK-CD-MS  
Fort Knox, KY 40121

**Commander**  
US Army Armor Center and Fort Knox  
ATTN: ATZK-CD-SD  
Fort Knox, KY 40121

Aerodyne Research Inc.  
ATTN: Dr. John F. Ebersole  
Crosby Drive  
Bedford, MA 01730

**Commander**  
Air Force Geophysics Laboratory  
ATTN: OPA (Dr. Robert W. Fenn)  
Hanscom AFB, MA 01731

**Commander**  
Air Force Geophysics Laboratory  
ATTN: OPI (Dr. Robert A. McClatchey)  
Hanscom AFB, MA 01731

Massachusetts Institute of Technology  
Lincoln Laboratory  
ATTN: Dr. T. J. Goblick, B-370  
P.O. Box 73  
Lexington, MA 02173

Massachusetts Institute of Technology  
Lincoln Laboratory  
ATTN: Dr. Michael Gruber  
P.O. Box 73  
Lexington, MA 02173

Raytheon Company  
Equipment Division  
ATTN: Dr. Charles M. Sonnenschein  
430 Boston Post Road  
Wayland, MA 01778

**Commander**  
US Army Ballistic Research Laboratory/  
ARRADCOM  
ATTN: DRDAR-BLB (Mr. Richard McGee)  
Aberdeen Proving Ground, MD 21005

**Commander/Director**  
Chemical Systems Laboratory  
US Army Armament Research  
& Development Command  
ATTN: DRDAR-CLB-PS (Dr. Edward Stuebing)  
Aberdeen Proving Ground, MD 21010

**Commander/Director**  
Chemical Systems Laboratory  
US Army Armament Research  
& Development Command  
ATTN: DRDAR-CLB-PS (Mr. Joseph Vervier)  
Aberdeen Proving Ground, MD 21010

**Commander/Director**  
Chemical Systems Laboratory  
US Army Armament Research  
& Development Command  
ATTN: DRDAR-CLY-A (Mr. Ronald Pennsyle)  
Aberdeen Proving Ground, MD 21010

**Commander**  
US Army Ballistic Research Laboratory/  
ARRADCOM  
ATTN: DRDAR-TSB-S (STINFO)  
Aberdeen Proving Ground, MD 21005

**Commander**  
US Army Electronics Research  
& Development Command  
ATTN: DRDEL-CCM (W. H. Pepper)  
Adelphi, MD 20783

**Commander**  
US Army Electronics Research  
& Development Command  
ATTN: DRDEL-CG/DRDEL-DC/DRDEL-CS  
2800 Powder Mill Road  
Adelphi, MD 20783

**Commander**  
US Army Electronics Research  
& Development Command  
ATTN: DRDEL-CT  
2800 Powder Mill Road  
Adelphi, MD 20783

**Commander**  
US Army Electronics Research  
& Development Command  
ATTN: DRDEL-PAO (M. Singleton)  
2800 Powder Mill Road  
Adelphi, MD 20783

**Project Manager**  
Smoke/Obscurants  
ATTN: DRDPM-SMK  
(Dr. Anthony Van de Wal, Jr.)  
Aberdeen Proving Ground, MD 21005

**Project Manager**  
Smoke/Obscurants  
ATTN: DRDPM-SMK-T (Mr. Sidney Gerard)  
Aberdeen Proving Ground, MD 21005

**Commander**  
US Army Test & Evaluation Command  
ATTN: DRSTE-AD-M (Mr. Warren M. Baity)  
Aberdeen Proving Ground, MD 21005

**Commander**  
US Army Test & Evaluation Command  
ATTN: DRSTE-AD-M (Dr. Norman E. Pentz)  
Aberdeen Proving Ground, MD 21005

**Director**  
US Army Materiel Systems Analysis Activity  
ATTN: DRXSY-AAM (Mr. William Smith)  
Aberdeen Proving Ground, MD 21005

**Director**  
US Army Materiel Systems Analysis Activity  
ATTN: DRXSY-CS (Mr. Philip H. Beavers)  
Aberdeen Proving Ground, MD 21005

**Director**  
US Army Materiel Systems Analysis Activity  
ATTN: DRXSY-GB (Wilbur L. Warfield)  
Aberdeen Proving Ground, MD 21005

**Director**  
US Army Materiel Systems Analysis Activity  
ATTN: DRXSY-GP (Mr. Fred Campbell)  
Aberdeen Proving Ground, MD 21005

**Director**  
US Army Materiel Systems Analysis Activity  
ATTN: DRXSY-GP (H. Stamper)  
Aberdeen Proving Grounds, MD 21005

**Director**  
US Army Materiel Systems Analysis Activity  
ATTN: DRXSY-GS  
(Mr. Michael Starks/Mr. Julian Chernick)  
Aberdeen Proving Ground, MD 21005

**Director**  
US Army Materiel Systems Analysis Activity  
ATTN: DRXSY-J (Mr. James F. O'Bryon)  
Aberdeen Proving Ground, MD 21005

**Director**  
US Army Materiel Systems Analysis Activity  
ATTN: DRXSY-LM (Mr. Robert M. Marchetti)  
Aberdeen Proving Ground, MD 21005

**Commander**  
Harry Diamond Laboratories  
ATTN: Dr. William W. Carter  
2800 Powder Mill Road  
Adelphi, MD 20783

**Commander**  
Harry Diamond Laboratories  
ATTN: DELHD-R-CM (Mr. Robert McCloskey)  
2800 Powder Mill Road  
Adelphi, MD 20783

**Commander**  
Harry Diamond Laboratories  
ATTN: DELHD-R-CM-NM (Dr. Robert Humphrey)  
2800 Powder Mill Road  
Adelphi, MD 20783

**Commander**  
Harry Diamond Laboratories  
ATTN: DELHD-R-CM-NM (Dr. Z. G. Sztankay)  
2800 Powder Mill Road  
Adelphi, MD 20783

**Commander**  
Harry Diamond Laboratories  
ATTN: DELHD-R-CM-NM (Dr. Joseph Nemarich)  
2800 Powder Mill Road  
Adelphi, MD 20783

**Commander**  
Air Force Systems Command  
ATTN: WER (Mr. Richard F. Picanso)  
Andrews AFB, MD 20334

**Martin Marietta Laboratories**  
ATTN: Jar Mo Chen  
1450 South Rolling Road  
Baltimore, MD 21227

**Commander**  
**US Army Concepts Analysis Agency**  
ATTN: CSCA-SMC (Mr. Hal E. Hock)  
8120 Woodmont Avenue  
Bethesda, MD 20014

**Director**  
**National Security Agency**  
ATTN: R52/Dr. Douglas Woods  
Fort George G. Meade, MD 20755

**Chief**  
**Intelligence Materiel Development**  
  **& Support Office**  
**US Army Electronic Warfare Laboratory**  
ATTN: DELEW-I (LTC Kenneth E. Thomas)  
Fort George G. Meade, MD 20755

**The Johns Hopkins University**  
**Applied Physics Laboratory**  
ATTN: Dr. Michael J. Lun  
John Hopkins Road  
Laurel, MD 20810

**Dr. Stephen T. Hanley**  
1720 Rhodesia Avenue  
Oxon Hill, MD 20022

**Science Applications Inc.**  
ATTN: Mr. G. D. Currie  
15 Research Drive  
Ann Arbor, MI 48103

**Science Applications Inc.**  
ATTN: Dr. Robert E. Turner  
15 Research Drive  
Ann Arbor, MI 48103

**Commander**  
**US Army Tank-Automotive Research**  
  **& Development Command**  
ATTN: DRDTA-ZSC (Mr. Harry Young)  
Warren, MI 48090

**Commander**  
**US Army Tank Automotive Research**  
  **& Development Command**  
ATTN: DRDTA-ZSC (Mr. Wallace Mick, Jr.)  
Warren, MI 48090

**Dr. A. D. Belmont**  
**Research Division**  
**Control Data Corporation**  
P.O. Box 1249  
Minneapolis, MN 55440

**Director**  
**US Army Engr Waterways Experiment Station**  
ATTN: WESEN (Mr. James Mason)  
P.O. Box 631  
Vicksburg, MS 39180

**Dr. Jerry Davis**  
**Department of Marine, Earth**  
  **and Atmospheric Sciences**  
**North Carolina State University**  
Raleigh, NC 27650

**Commander**  
**US Army Research Office**  
ATTN: DRXRO-GS (Dr. Leo Alpert)  
P.O. Box 12211  
Research Triangle Park, NC 27709

**Commander**  
**US Army Research Office**  
ATTN: DRXRO-PP (Brenda Mann)  
P.O. Box 12211  
Research Triangle Park, NC 27709

**Commander**  
**US Army Cold Regions Research**  
  **& Engineering Laboratory**  
ATTN: CRREL-RD (Dr. K. F. Sterrett)  
Hanover, NH 03755

**Commander/Director**  
**US Army Cold Regions Research**  
  **& Engineering Laboratory**  
ATTN: CRREL-RG (Mr. George Aitken)  
Hanover, NH 03755

**Commander**  
**US Army Cold Regions Research**  
  **& Engineering Laboratory**  
ATTN: CRREL-RG (Mr. Roger H. Berger)  
Hanover, NH 03755

**Commander**  
**US Army Armament Research**  
  **& Development Command**  
ATTN: DRDAR-AC (Mr. James Greenfield)  
Dover, NJ 07801

**Commander**  
US Army Armament Research  
& Development Command  
ATTN: DRDAR-TS (Ring #59)  
Dover, NJ 07801

**Commander**  
US Army Armament Research  
& Development Command  
ATTN: DRCPM-CAWS-SI (Mr. Peteris Jansons)  
Dover, NJ 07801

**Commander**  
US Army Armament Research  
& Development Command  
ATTN: DRCPM-CARH-SI (Mr. C. H. Waldron)  
Dover, NJ 07801

**Deputy Joint Project Manager**  
for Navy/JSMC SAL (Go)  
ATTN: DRCPM-CAWS-NV (CPT Joseph Micelli)  
Dover, NJ 07801

**Commander/Director**  
US Army Combat Surveillance & Target  
Acquisition Laboratory  
ATTN: DELCS-1 (Mr. David Longinotti)  
Fort Monmouth, NJ 07703

**Commander/Director**  
US Army Combat Surveillance & Target  
Acquisition Laboratory  
ATTN: DELCS-PE (Mr. Ben A. Di Campi)  
Fort Monmouth, NJ 07703

**Commander/Director**  
US Army Combat Surveillance & Target  
Acquisition Laboratory  
ATTN: DELCS-R-S (Mr. Donald L. Fciani)  
Fort Monmouth, NJ 07703

**Director**  
US Army Electronics Technology &  
Devices Laboratory  
ATTN: DELET-DD (S. Danko)  
Fort Monmouth, NJ 07703

**Project Manager**  
FIREFINDER/REMBASS  
ATTN: DRCPM-FFR-TM (Mr. John M. Bialo)  
Fort Monmouth, NJ 07703

**Commander**  
US Army Electronics Research  
& Development Command  
ATTN: DRER-1A (Dr. Walter S. McAfee)  
Fort Monmouth, NJ 07703

**Director**  
USA TRADOC Systems Analysis Activity  
ATTN: ATAA-1A  
White Sands Missile Range, NM 88002

**Director**  
USA TRADOC Systems Analysis Activity  
ATTN: ATAA-1B  
White Sands Missile Range, NM 88002

**Director**  
USA TRADOC Systems Analysis Activity  
ATTN: ATAA-1C  
White Sands Missile Range, NM 88002

**Director**  
USA TRADOC Systems Analysis Activity  
ATTN: ATAA-1D (Mr. Louie Dominguez)  
White Sands Missile Range, NM 88002

**Director**  
USA TRADOC Systems Analysis Activity  
ATTN: ATAA-1D (Mr. William J. Leach)  
White Sands Missile Range, NM 88002

**Director**  
USA TRADOC Systems Analysis Activity  
ATTN: ATAA-1E (Mr. Roger F. Willis)  
White Sands Missile Range, NM 88002

**Director**  
Office of Missle Electronic Warfare  
ATTN: DRXDF-SD (Dr. Steven Kovel)  
White Sands Missile Range, NM 88002

**Office of the Test Director**  
Joint Services EO GW CM Test Program  
ATTN: DRXDF-TD (Mr. Welton Findley)  
White Sands Missile Range, NM 88002

**Commander**  
US Army White Sands Missile Range  
ATTN: STEWS-PT-AL (Laurel B. Saunders)  
White Sands Missile Range, NM 88002

**Commander**  
US Army R&D Coordinator  
US Embassy - Bonn  
Box 165  
APO New York 09080

**Grumman Aerospace Corporation**  
Research Department - MS A08-35  
ATTN: John E. A. Selby  
Bethpage, NY 11714

**Rome Air Development Center**  
ATTN: Documents Library  
TSLD (Bette Smith)  
Griffiss AFB, NY 13441

**Dr. Roberto Vaglio-Laurin**  
Faculty of Arts and Science  
Dept. of Applied Science  
26-36 Stuyvesant Street  
New York, NY 10003

**Air Force Wright Aeronautical Laboratories/**  
Avionics Laboratory  
ATTN: AFWAL/AARI-3 (Mr. Harold Geltmacher)  
Wright-Patterson AFB, OH 45433

**Air Force Wright Aeronautical Laboratories/**  
Avionics Laboratory  
ATTN: AFWAL/AARI-3 (CPT William C. Smith)  
Wright-Patterson AFB, OH 45433

**Commandant**  
US Army Field Artillery School  
ATTN: ATSF-CF-R (CPT James M. Watson)  
Fort Sill, OK 73503

**Commandant**  
US Army Field Artillery School  
ATTN: ATSF-CD-MS  
Fort Sill, OK 73503

**Commandant**  
US Army Field Artillery School  
ATTN: ATSF-CF-R  
Fort Sill, OK 73503

**Commandant**  
US Army Field Artillery School  
ATTN: NOAA Liaison Officer  
(CDR Jeffrey G. Carlen)  
Fort Sill, OK 73503

**Commandant**  
US Army Field Artillery School  
Morris Swett Library  
ATTN: Reference Librarian  
Fort Sill, OK 73503

**Commander**  
Naval Air Development Center  
ATTN: File 301 (Mr. George F. Eck)  
Warminster, PA 18974

**The University of Texas at El Paso**  
Electrical Engineering Department  
ATTN: Dr. Joseph H. Pierluissi  
El Paso, TX 79968

**Commandant**  
US Army Air Defense School  
ATTN: ATSA-CD-SC-A (CPT Charles T. Thorn)  
Fort Bliss, TX 79916

**Commander**  
HQ, TRADOC Combined Arms Test Activity  
ATTN: ATCAT-OP-Q (CPT Henry C. Cobb, Jr.)  
Fort Hood, TX 76544

**Commander**  
HQ, TRADOC Combined Arms Test Activity  
ATTN: ATCAT-SCI (Dr. Darrell W. Collier)  
Fort Hood, TX 76544

**Commander**  
US Army Dugway Proving Ground  
ATTN: STEDP-MT-DA-L  
Dugway, UT 84022

**Commander**  
US Army Dugway Proving Ground  
ATTN: STEDP-MT-DA-M (Mr. Paul E. Carlson)  
Dugway, UT 84022

**Commander**  
US Army Dugway Proving Ground  
ATTN: STEDP-MT-DA-T (Mr. John Trethewey)  
Dugway, UT 84022

**Commander**  
US Army Dugway Proving Ground  
ATTN: STEDP-MT-DA-T (Mr. William Peterson)  
Dugway, UT 84022

Defense Documentation Center

ATTN: DDC-TCA  
Cameron Station Bldg 5  
Alexandria, VA 22314  
12

Ballistic Missile Defense Program Office  
ATTN: DACS-BMT (Colonel Harry F. Ennis)  
5001 Eisenhower Avenue  
Alexandria, VA 22333

Defense Technical Information Center  
ATTN: DDA-2 (Mr. James F. Shafer)  
Cameron Station, Bldg 5  
Alexandria, VA 22314

Commander  
US Army Materiel Development  
& Readiness Command  
ATTN: DRCRSI-EE (Mr. Albert Giambalvo)  
5001 Eisenhower Avenue  
Alexandria, VA 22333

Commander  
US Army Materiel Development  
& Readiness Command  
ATTN: DRCLDC (Mr. James Bender)  
5001 Eisenhower Avenue  
Alexandria, VA 22333

Defense Advanced Rsch Projects Agency  
ATTN: Steve Zakanyez  
1400 Wilson Blvd  
Arlington, VA 22209

Defense Advanced Rsch Projects Agency  
ATTN: Dr. James Tegnelia  
1400 Wilson Blvd  
Arlington, VA 22209

Institute for Defense Analyses  
ATTN: Mr. Lucien M. Biberman  
400 Army-Navy Drive  
Arlington, VA 22202

Institute for Defense Analyses  
ATTN: Dr. Ernest Bauer  
400 Army-Navy Drive  
Arlington, VA 22202

Institute for Defense Analyses  
ATTN: Dr. Hans G. Wolfhard  
400 Army-Navy Drive  
Arlington, VA 22202

System Planning Corporation  
ATTN: Mr. Daniel Friedman  
1500 Wilson Boulevard  
Arlington, VA 22209

System Planning Corporation  
ATTN: COL Hank Shelton  
1500 Wilson Boulevard  
Arlington, VA 22209

US Army Intelligence & Security Command  
ATTN: Edwin Speakman, Scientific Advisor  
Arlington Hall Station  
Arlington, VA 22212

Commander  
US Army Operational Test  
& Evaluation Agency  
ATTN: CSTE-ED (Mr. Floyd I. Hill)  
5600 Columbia Pike  
Falls Church, VA 22041

Commander and Director  
US Army Engineer Topographic Laboratories  
ATTN: ETL-GS-A (Mr. Thomas Neidringhaus)  
Fort Belvoir, VA 22060

Director  
US Army Night Vision &  
Electro-Optics Laboratory  
ATTN: DELNV-L (Dr. Rudolf G. Buser)  
Fort Belvoir, VA 22060

Director  
US Army Night Vision &  
Electro-Optics Laboratory  
ATTN: DELNV-L (Dr. Robert S. Rodhe)  
Fort Belvoir, VA 22060

Director  
US Army Night Vision &  
Electro-Optics Laboratory  
ATTN: DELNV-VI (Mr. Joseph R. Moulton)  
Fort Belvoir, VA 22060

Director  
US Army Night Vision &  
Electro-Optics Laboratory  
ATTN: DELNV-VI (Luanne P. Obert)  
Fort Belvoir, VA 22060

Director  
US Army Night Vision & Electro-Optics Laboratory  
ATTN: DELNV-VI (Mr. Thomas W. Cassidy)  
Fort Belvoir, VA 22060

Director  
US Army Night Vision & Electro-Optics Laboratory  
ATTN: DELNV-VI (Mr. Richard J. Bergemann)  
Fort Belvoir, VA 22060

Director  
US Army Night Vision & Electro-Optics Laboratory  
ATTN: DELNV-VI (Dr. James A. Ratches)  
Fort Belvoir, VA 22060

Commander  
US Army Training & Doctrine Command  
ATTN: ATCD-AN  
Fort Monroe, VA 23651

Commander  
US Army Training & Doctrine Command  
ATTN: ATCD-AN-M  
Fort Monroe, VA 23651

Commander  
US Army Training & Doctrine Command  
ATTN: ATCD-F-A (Mr. Chris O'Connor, Jr.)  
Fort Monroe, VA 23651

Commander  
US Army Training & Doctrine Command  
ATTN: ATCD-IE-R (Mr. David M. Ingram)  
Fort Monroe, VA 23651

Commander  
US Army Training & Doctrine Command  
ATTN: ATCD-M-I/ATCD-M-A  
Fort Monroe, VA 23651

Commander  
US Army Training & Doctrine Command  
ATTN: ATDOC-TA (Dr. Marvin P. Pastell)  
Fort Monroe, VA 23651

Department of the Air Force  
OL-I, AWS  
Fort Monroe, VA 23651

Department of the Air Force  
HQs 5 Weather Wing (MAC)  
ATTN: 5 WW/DN  
Langley Air Force Base, VA 23655

Commander  
US Army INSCOM/Quest Research Corporation  
ATTN: Mr. Donald Wilmot  
6845 Elm Street, Suite 407  
McLean, VA 22101

General Research Corporation  
ATTN: Dr. Ralph Zirkind  
7655 Old Springhouse Road  
McLean, VA 22102

Science Applications, Inc.  
8400 Westpark Drive  
ATTN: Dr. John E. Cockayne  
McLean, VA 22102

US Army Nuclear & Chemical Agency  
ATTN: MONA-WE (Dr. John A. Berberet)  
7500 Backlick Road, Bldg 2073  
Springfield, VA 22150

Director  
US Army Signals Warfare Laboratory  
ATTN: DELSW-EA (Mr. Douglas Harkleroad)  
Vint Hill Farms Station  
Warrenton, VA 22186

Director  
US Army Signals Warfare Laboratory  
ATTN: DELSW-OS (Dr. Royal H. Burkhardt)  
Vint Hill Farms Station  
Warrenton, VA 22186

Commander  
US Army Cold Regions Test Center  
ATTN: STECR-TD (Mr. Jerold Barger)  
APO Seattle, WA 98733

HQDA (SAUS-OR/Hunter M. Woodall, Jr./  
Dr. Herbert K. Fallin)  
Rm 2E 614, Pentagon  
Washington, DC 20301

COL Elbert W. Friday, Jr.  
OUSDRE  
Rm 3D 129, Pentagon  
Washington, DC 20301

Defense Communications Agency  
Technical Library Center  
Code 222  
Washington, DC 20305

Director  
Defense Nuclear Agency  
ATTN: Technical Library (Mrs. Betty Fox)  
Washington, DC 20305

Director  
Defense Nuclear Agency  
ATTN: RAAE (Dr. Carl Fitz)  
Washington, DC 20305

Director  
Defense Nuclear Agency  
ATTN: SPAS (Mr. Donald J. Kohler)  
Washington, DC 20305

Defense Intelligence Agency  
ATTN: DT/AC (LTC Robert Poplawski)  
Washington, DC 20301

HQDA (DAMA-ARZ-D/Dr. Verderame)  
Washington, DC 20310

HQDA (DAMI-ISP/Mr. Beck)  
Washington, DC 20310

Department of the Army  
Deputy Chief of Staff for  
Operations and Plans  
ATTN: DAMO-RQ  
Washington, DC 20310

Department of the Army  
Director of Telecommunications and  
Command and Control  
ATTN: DAMO-TCZ  
Washington, DC 20310

Department of the Army  
Assistant Chief of Staff for Intelligence  
ATTN: DAMI-TS  
Washington, DC 20310

HQDA (DAEN-RDM/Dr. de Percin)  
Casimir Pulaski Building  
20 Massachusetts Avenue  
Room 6203  
Washington, DC 20314

National Science Foundation  
Division of Atmospheric Sciences  
ATTN: Dr. Eugene W. Bierly  
1800 G. Street, N.W.  
Washington, DC 20550

Director  
Naval Research Laboratory  
ATTN: Code 4320 (Dr. Lothar H. Ruhnke)  
Washington, DC 20375

Commanding Officer  
Naval Research Laboratory  
ATTN: Code 6002 (Dr. John MacCallum, Jr.)  
Washington, DC 20375

Commanding Officer  
Naval Research Laboratory  
ATTN: Code 6530 (Mr. Raymond A. Patten)  
Washington, DC 20375

Commanding Officer  
Naval Research Laboratory  
ATTN: Code 6533 (Dr. James A. Dowling)  
Washington, DC 20375

ATMOSPHERIC SCIENCES RESEARCH REPORTS

1. Lindberg, J. D. 'An Improvement to a Method for Measuring the Absorption Coefficient of Atmospheric Dust and other Strongly Absorbing Powders," ECOM-5565, July 1975.
2. Avara, Elton P., "Mesoscale Wind Shears Derived from Thermal Winds," ECOM-5566, July 1975.
3. Gomez, Richard B., and Joseph H. Pierluissi, "Incomplete Gamma Function Approximation for King's Strong-Line Transmittance Model," ECOM-5567, July 1975.
4. Blanco, A. J., and B. F. Engebos, "Ballistic Wind Weighting Functions for Tank Projectiles," ECOM-5568, August 1975.
5. Taylor, Fredrick J., Jack Smith, and Thomas H. Pries, "Crosswind Measurements through Pattern Recognition Techniques," ECOM-5569, July 1975.
6. Walters, D. L., "Crosswind Weighting Functions for Direct-Fire Projectiles," ECOM-5570, August 1975.
7. Duncan, Louis D., "An Improved Algorithm for the Iterated Minimal Information Solution for Remote Sounding of Temperature," ECOM-5571, August 1975.
8. Robbiani, Raymond L., "Tactical Field Demonstration of Mobile Weather Radar Set AN/TPS-41 at Fort Rucker, Alabama," ECOM-5572, August 1975.
9. Miers, B., G. Blackman, D. Langer, and N. Lorimier, "Analysis of SMS/GOES Film Data," ECOM-5573, September 1975.
10. Manquero, Carlos, Louis Duncan, and Rufus Bruce, "An Indication from Satellite Measurements of Atmospheric CO<sub>2</sub> Variability," ECOM-5574, September 1975.
11. Petracca, Carmine, and James D. Lindberg, "Installation and Operation of an Atmospheric Particulate Collector," ECOM-5575, September 1975.
12. Avara, Elton P., and George Alexander, "Empirical Investigation of Three Iterative Methods for Inverting the Radiative Transfer Equation," ECOM-5576, October 1975.
13. Alexander, George D., "A Digital Data Acquisition Interface for the SMS Direct Readout Ground Station - Concept and Preliminary Design," ECOM-5577, October 1975.
14. Cantor, Israel, "Enhancement of Point Source Thermal Radiation Under Clouds in a Nonattenuating Medium," ECOM-5578, October 1975.

15. Norton, Colburn, and Glenn Hoidal, "The Diurnal Variation of Mixing Height by Month over White Sands Missile Range, NM," ECOM-5579, November 1975.
16. Avara, Elton P., "On the Spectrum Analysis of Binary Data," ECOM-5580, November 1975.
17. Taylor, Fredrick J., Thomas H. Pries, and Chao-Huan Huang, "Optimal Wind Velocity Estimation," ECOM-5581, December 1975.
18. Avara, Elton P., "Some Effects of Autocorrelated and Cross-Correlated Noise on the Analysis of Variance," ECOM-5582, December 1975.
19. Gillespie, Patti S., R. L. Armstrong, and Kenneth O. White, "The Spectral Characteristics and Atmospheric  $\text{CO}_2$  Absorption of the  $\text{Ho}^{+3}:\text{YLF}$  Laser at  $2.05\mu\text{m}$ ," ECOM-5583, December 1975.
20. Novlan, David J., "An Empirical Method of Forecasting Thunderstorms for the White Sands Missile Range," ECOM-5584, February 1976.
21. Avara, Elton P., "Randomization Effects in Hypothesis Testing with Autocorrelated Noise," ECOM-5585, February 1976.
22. Watkins, Wendell R., "Improvements in Long Path Absorption Cell Measurement," ECOM-5586, March 1976.
23. Thomas, Joe, George D. Alexander, and Marvin Dubbin, "SATTEL - An Army Dedicated Meteorological Telemetry System," ECOM-5587, March 1976.
24. Kennedy, Bruce W., and Delbert Bynum, "Army User Test Program for the RDT&E-XM-75 Meteorological Rocket," ECOM-5588, April 1976.
25. Barnett, Kenneth M., "A Description of the Artillery Meteorological Comparisons at White Sands Missile Range, October 1974 - December 1974 ('PASS' - Prototype Artillery [Meteorological] Subsystem)," ECOM-5589, April 1976.
26. Miller, Walter B., "Preliminary Analysis of Fall-of-Shot From Project 'PASS'," ECOM-5590, April 1976.
27. Avara, Elton P., "Error Analysis of Minimum Information and Smith's Direct Methods for Inverting the Radiative Transfer Equation," ECOM-5591, April 1976.
28. Yee, Young P., James D. Horn, and George Alexander, "Synoptic Thermal Wind Calculations from Radiosonde Observations Over the Southwestern United States," ECOM-5592, May 1976.

29. Duncan, Louis D., and Mary Ann Seagraves, "Applications of Empirical Corrections to NOAA-4 VTPR Observations," ECOM-5593, May 1976.
30. Miers, Bruce T., and Steve Weaver, "Applications of Meteorological Satellite Data to Weather Sensitive Army Operations," ECOM-5594, May 1976.
31. Sharenow, Moses, "Redesign and Improvement of Balloon ML-566," ECOM-5595, June 1976.
32. Hansen, Frank V., "The Depth of the Surface Boundary Layer," ECOM-5596, June 1976.
33. Pinnick, R. G., and E. B. Stenmark, "Response Calculations for a Commerical Light-Scattering Aerosol Counter," ECOM-5597, July 1976.
34. Mason, J., and G. B. Hoidal, "Visibility as an Estimator of Infrared Transmittance," ECOM-5598, July 1976.
35. Bruce, Rufus E., Louis D. Duncan, and Joseph H. Pierluissi, "Experimental Study of the Relationship Between Radiosonde Temperatures and Radiometric-Area Temperatures," ECOM-5599, August 1976.
36. Duncan, Louis D., "Stratospheric Wind Shear Computed from Satellite Thermal Sounder Measurements," ECOM-5800, September 1976.
37. Taylor, F., P. Mohan, P. Joseph, and T. Pries, "An All Digital Automated Wind Measurement System," ECOM-5801, September 1976.
38. Bruce, Charles, "Development of Spectrophones for CW and Pulsed Radiation Sources," ECOM-5802, September 1976.
39. Duncan, Louis D., and Mary Ann Seagraves, "Another Method for Estimating Clear Column Radiances," ECOM-5803, October 1976.
40. Blanco, Abel J., and Larry E. Taylor, "Artillery Meteorological Analysis of Project Pass," ECOM-5804, October 1976.
41. Miller, Walter, and Bernard Engebos, "A Mathematical Structure for Refinement of Sound Ranging Estimates," ECOM-5805, November 1976.
42. Gillespie, James B., and James D. Lindberg, "A Method to Obtain Diffuse Reflectance Measurements from 1.0 and 3.0 $\mu$ m Using a Cary 171 Spectrophotometer," ECOM-5806, November 1976.
43. Rubio, Roberto, and Robert O. Olsen, "A Study of the Effects of Temperature Variations on Radio Wave Absorption," ECOM-5807, November 1976.

44. Ballard, Harold N., "Temperature Measurements in the Stratosphere from Balloon-Borne Instrument Platforms, 1968-1975," ECOM-5808, December 1976.
45. Monahan, H. H., "An Approach to the Short-Range Prediction of Early Morning Radiation Fog," ECOM-5809, January 1977.
46. Engebos, Bernard Francis, "Introduction to Multiple State Multiple Action Decision Theory and Its Relation to Mixing Structures," ECOM-5810, January 1977.
47. Low, Richard D. H., "Effects of Cloud Particles on Remote Sensing from Space in the 10-Micrometer Infrared Region," ECOM-5811, January 1977.
48. Bonner, Robert S., and R. Newton, "Application of the AN/GVS-5 Laser Rangefinder to Cloud Base Height Measurements," ECOM-5812, February 1977.
49. Rubio, Roberto, "Lidar Detection of Subvisible Reentry Vehicle Erosive Atmospheric Material," ECOM-5813, March 1977.
50. Low, Richard D. H., and J. D. Horn, "Mesoscale Determination of Cloud-Top Height: Problems and Solutions," ECOM-5814, March 1977.
51. Duncan, Louis D., and Mary Ann Seagraves, "Evaluation of the NOAA-4 VTPR Thermal Winds for Nuclear Fallout Predictions," ECOM-5815, March 1977.
52. Randhawa, Jagir S., M. Izquierdo, Carlos McDonald, and Zvi Salpeter, "Stratospheric Ozone Density as Measured by a Chemiluminescent Sensor During the Stratcom VI-A Flight," ECOM-5816, April 1977.
53. Rubio, Roberto, and Mike Izquierdo, "Measurements of Net Atmospheric Irradiance in the 0.7- to 2.8-Micrometer Infrared Region," ECOM-5817, May 1977.
54. Ballard, Harold N., Jose M. Serna, and Frank P. Hudson, Consultant for Chemical Kinetics, "Calculation of Selected Atmospheric Composition Parameters for the Mid-Latitude, September Stratosphere," ECOM-5818, May 1977.
55. Mitchell, J. D., R. S. Sagar, and R. J. Olsen, "Positive Ions in the Middle Atmosphere During Sunrise Conditions," ECOM-5919, May 1977.
56. White, Kenneth O., Wendell R. Watkins, Stuart A. Schleusener, and Ronald L. Johnson, "Solid-State Laser Wavelength Identification Using a Reference Absorber," ECOM-5820, June 1977.
57. Watkins, Wendell R., and Richard G. Dixon, "Automation of Long-Path Absorption Cell Measurements," ECOM-5821, June 1977.

58. Taylor, S. E., J. M. Davis, and J. B. Mason, "Analysis of Observed Soil Skin Moisture Effects on Reflectance," ECOM-5822, June 1977.
59. Duncan, Louis D., and Mary Ann Seagraves, "Fallout Predictions Computed from Satellite Derived Winds," ECOM-5823, June 1977.
60. Snider, D. E., D. G. Murcray, F. H. Murcray, and W. J. Williams, "Investigation of High-Altitude Enhanced Infrared Background Emissions," (U), SECRET, ECOM-5824, June 1977.
61. Dubbin, Marvin H., and Dennis Hall, "Synchronous Meteorological Satellite Direct Readout Ground System Digital Video Electronics," ECOM-5825, June 1977.
62. Miller, W., and B. Engebos, "A Preliminary Analysis of Two Sound Ranging Algorithms," ECOM-5826, July 1977.
63. Kennedy, Bruce W., and James K. Luers, "Ballistic Sphere Techniques for Measuring Atmospheric Parameters," ECOM-5827, July 1977.
64. Duncan, Louis D., "Zenith Angle Variation of Satellite Thermal Sounder Measurements," ECOM-5828, August 1977.
65. Hansen, Frank V., "The Critical Richardson Number," ECOM-5829, September 1977.
66. Ballard, Harold N., and Frank P. Hudson (Compilers), "Stratospheric Composition Balloon-Borne Experiment," ECOM-5830, October 1977.
67. Barr, William C., and Arnold C. Peterson, "Wind Measuring Accuracy Test of Meteorological Systems," ECOM-5831, November 1977.
68. Ethridge, G. A., and F. V. Hansen, "Atmospheric Diffusion: Similarity Theory and Empirical Derivations for Use in Boundary Layer Diffusion Problems," ECOM-5832, November 1977.
69. Low, Richard D. H., "The Internal Cloud Radiation Field and a Technique for Determining Cloud Blackness," ECOM-5833, December 1977.
70. Watkins, Wendell R., Kenneth O. White, Charles W. Bruce, Donald L. Walters, and James D. Lindberg, "Measurements Required for Prediction of High Energy Laser Transmission," ECOM-5834, December 1977.
71. Rubio, Robert, "Investigation of Abrupt Decreases in Atmospherically Backscattered Laser Energy," ECOM-5835, December 1977.
72. Monahan, H. H., and R. M. Cionco, "An Interpretative Review of Existing Capabilities for Measuring and Forecasting Selected Weather Variables (Emphasizing Remote Means)," ASL-TR-0001, January 1978.

73. Heaps, Melvin G., "The 1979 Solar Eclipse and Validation of D-Region Models," ASL-TR-0002, March 1978.
74. Jennings, S. G., and J. B. Gillespie, "M.I.F. Theory Sensitivity Studies - The Effects of Aerosol Complex Refractive Index and Size Distribution Variations on Extinction and Absorption Coefficients, Part II: Analysis of the Computational Results," ASL-TR-0003, March 1978.
75. White, Kenneth O., et al, "Water Vapor Continuum Absorption in the 3.5 $\mu$ m to 4.0 $\mu$ m Region," ASL-TR-0004, March 1978.
76. Olsen, Robert O., and Bruce W. Kennedy, "ABRES Pretest Atmospheric Measurements," ASL-TR-0005, April 1978.
77. Ballard, Harold N., Jose M. Serna, and Frank P. Hudson, "Calculation of Atmospheric Composition in the High Latitude September Stratosphere," ASL-TR-0006, May 1978.
78. Watkins, Wendell R., et al, "Water Vapor Absorption Coefficients at HF Laser Wavelengths," ASL-TR-0007, May 1978.
79. Hansen, Frank V., "The Growth and Prediction of Nocturnal Inversions," ASL-TR-0008, May 1978.
80. Samuel, Christine, Charles Bruce, and Ralph Brewer, "Spectrophone Analysis of Gas Samples Obtained at Field Site," ASL-TR-0009, June 1978.
81. Pinnick, R. G., et al., "Vertical Structure in Atmospheric Fog and Haze and its Effects on IR Extinction," ASL-TR-0010, July 1978.
82. Low, Richard D. H., Louis D. Duncan, and Richard B. Gomez, "The Microphysical Basis of Fog Optical Characterization," ASL-TR-0011, August 1978.
83. Heaps, Melvin G., "The Effect of a Solar Proton Event on the Minor Neutral Constituents of the Summer Polar Mesosphere," ASL-TR-0012, August 1978.
84. Mason, James B., "Light Attenuation in Falling Snow," ASL-TR-0013, August 1978.
85. Blanco, Abel J., "Long-Range Artillery Sound Ranging: 'PASS' Meteorological Application," ASL-TR-0014, September 1978.
86. Heaps, M. G., and F. E. Niles, "Modeling of Ion Chemistry of the D-Region: A Case Study Based Upon the 1966 Total Solar Eclipse," ASL-TR-0015, September 1978.

87. Jennings, S. G., and R. G. Pinnick, "Effects of Particulate Complex Refractive Index and Particle Size Distribution Variations on Atmospheric Extinction and Absorption for Visible Through Middle-Infrared Wavelengths," ASL-TR-0016, September 1978.
88. Watkins, Wendell R., Kenneth O. White, Lanny R. Bower, and Brian Z. Sojka, "Pressure Dependence of the Water Vapor Continuum Absorption in the 3.5- to 4.0-Micrometer Region," ASL-TR-0017, September 1978.
89. Miller, W. B., and B. F. Engebos, "Behavior of Four Sound Ranging Techniques in an Idealized Physical Environment," ASL-TR-0018, September 1978.
90. Gomez, Richard G., "Effectiveness Studies of the CBU-88/B Bomb, Cluster, Smoke Weapon," (U), CONFIDENTIAL ASL-TR-0019, September 1978.
91. Miller, August. Richard C. Shirkey, and Mary Ann Seagraves, "Calculation of Thermal Emission from Aerosols Using the Doubling Technique," ASL-TR-0020, November 1978.
92. Lindberg, James D., et al, "Measured Effects of Battlefield Dust and Smoke on Visible, Infrared, and Millimeter Wavelengths Propagation: A Preliminary Report on Dusty Infrared Test-I (DIRT-I)," ASL-TR-0021, January 1979.
93. Kennedy, Bruce W., Arthur Kinghorn, and B. R. Hixon, "Engineering Flight Tests of Range Meteorological Sounding System Radiosonde," ASL-TR-0022, February 1979.
94. Rubio, Roberto, and Don Hock, "Microwave Effective Earth Radius Factor Variability at Wiesbaden and Balboa," ASL-TR-0023, February 1979.
95. Low, Richard D. H., "A Theoretical Investigation of Cloud/Fog Optical Properties and Their Spectral Correlations," ASL-TR-0024, February 1979.
96. Pinnick, R. G., and H. J. Auvermann, "Response Characteristics of Knollenberg Light-Scattering Aerosol Counters," ASL-TR-0025, February 1979.
97. Heaps, Melvin G., Robert O. Olsen, and Warren W. Berning, "Solar Eclipse 1979, Atmospheric Sciences Laboratory Program Overview," ASL-TR-0026, February 1979.
98. Blanco, Abel J., "Long-Range Artillery Sound Ranging: 'PASS' GR-8 Sound Ranging Data," ASL-TR-0027, March 1979.
99. Kennedy, Bruce W., and Jose M. Serna, "Meteorological Rocket Network System Reliability," ASL-TR-0028, March 1979.

100. Swingle, Donald M., "Effects of Arrival Time Errors in Weighted Range Equation Solutions for Linear Base Sound Ranging," ASL-TR-0029, April 1979.
101. Umstead, Robert K., Ricardo Pena, and Frank V. Hansen, "KWIK: An Algorithm for Calculating Munition Expenditures for Smoke Screening/Obscuration in Tactical Situations," ASL-TR-0030, April 1979.
102. D'Arcy, Edward M., "Accuracy Validation of the Modified Nike Hercules Radar," ASL-TR-0031, May 1979.
103. Rodriguez, Ruben, "Evaluation of the Passive Remote Crosswind Sensor," ASL-TR-0032, May 1979.
104. Barber, T. L., and R. Rodriguez, "Transit Time Lidar Measurement of Near-Surface Winds in the Atmosphere," ASL-TR-0033, May 1979.
105. Low, Richard D. H., Louis D. Duncan, and Y. Y. Roger R. Hsiao, "Microphysical and Optical Properties of California Coastal Fogs at Fort Ord," ASL-TR-0034, June 1979.
106. Rodriguez, Ruben, and William J. Vechione, "Evaluation of the Saturation Resistant Crosswind Sensor," ASL-TR-0035, July 1979.
107. Ohmstede, William D., "The Dynamics of Material Layers," ASL-TR-0036, July 1979.
108. Pinnick, R. G., S. G. Jennings, Petr Chylek, and H. J. Auermann, "Relationships between IR Extinction Absorption, and Liquid Water Content of Fogs," ASL-TR-0037, August 1979.
109. Rodriguez, Ruben, and William J. Vechione, "Performance Evaluation of the Optical Crosswind Profiler," ASL-TR-0038, August 1979.
110. Miers, Bruce T., "Precipitation Estimation Using Satellite Data," ASL-TR-0039, September 1979.
111. Dickson, David H., and Charles M. Sonnenschein, "Helicopter Remote Wind Sensor System Description," ASL-TR-0040, September 1979.
112. Heaps, Melvin G., and Joseph M. Heimerl, "Validation of the Dairchem Code, I: Quiet Midlatitude Conditions," ASL-TR-0041, September 1979.
113. Bonner, Robert S., and William J. Lentz, "The Visioceilometer: A Portable Cloud Height and Visibility Indicator," ASL-TR-0042, October 1979.
114. Cohn, Stephen L., "The Role of Atmospheric Sulfates in Battlefield Obscurations," ASL-TR-0043, October 1979.

115. Fawbush, E. J., et al, "Characterization of Atmospheric Conditions at the High Energy Laser System Test Facility (HELSTF), White Sands Missile Range, New Mexico, Part I, 24 March to 8 April 1977," ASL-TR-0044, November 1979.
116. Barber, Ted L., "Short-Time Mass Variation in Natural Atmospheric Dust," ASL-TR-0045, November 1979.
117. Low, Richard D. H., "Fog Evolution in the Visible and Infrared Spectral Regions and its Meaning in Optical Modeling," ASL-TR-0046, December 1979.
118. Duncan, Louis D., et al, "The Electro-Optical Systems Atmospheric Effects Library, Volume I: Technical Documentation," ASL-TR-0047, December 1979.
119. Shirkey, R. C., et al, "Interim E-0 SAEL, Volume II, Users Manual," ASL-TR-0048, December 1979.
120. Kobayashi, H. K., "Atmospheric Effects on Millimeter Radio Waves," ASL-TR-0049, January 1980.
121. Seagraves, Mary Ann, and Louis D. Duncan, "An Analysis of Transmittances Measured Through Battlefield Dust Clouds," ASL-TR-0050, February 1980.
122. Dickson, David H., and Jon E. Ottesen, "Helicopter Remote Wind Sensor Flight Test," ASL-TR-0051, February 1980.
123. Pinnick, R. G., and S. G. Jennings, "Relationships Between Radiative Properties and Mass Content of Phosphoric Acid, HC, Petroleum Oil, and Sulfuric Acid Military Smokes," ASL-TR-0052, April 1980.
124. Hinds, B. D., and J. B. Gillespie, "Optical Characterization of Atmospheric Particulates on San Nicolas Island, California," ASL-TR-0053, April 1980.
125. Miers, Bruce T., "Precipitation Estimation for Military Hydrology," ASL-TR-0054, April 1980.
126. Stenmark, Ernest B., "Objective Quality Control of Artillery Computer Meteorological Messages," ASL-TR-0055, April 1980.
127. Duncan, Louis D., and Richard D. H. Low, "Bimodal Size Distribution Models for Fogs at Meppen, Germany," ASL-TR-0056, April 1980.
128. Olsen, Robert O., and Jagir S. Randhawa, "The Influence of Atmospheric Dynamics on Ozone and Temperature Structure," ASL-TR-0057, May 1980.

129. Kennedy, Bruce W., et al, "In-Situ Interferent Test-II (SIRT-II) Program," ASL-TR-0062, May 1980.
130. Heaps, Melvin G., Robert P. Miller, Warren Berling, John Gross, and Arthur J. Grossman, "1979 Solar Eclipse, Part I - Atmospheric Observances Laboratory Field Program Summary," ASL-TR-0063, May 1980.
131. Miller, Walter R., and Bruce W. Kennedy, "Acoustical Absorption Coefficients for Two (PTAP-1, 2) Photoacoustic Chambers," ASL-TR-0064, June 1980.
132. Holt, E. H., editor, "Atmospheric Dust: Measurements for Dust Absorption and Obscuration Applications," ASL-TR-0065, June 1980.
133. Shirkey, Richard C., August Miller, George W. Goedecke, and Rudal Rehi, "Single Scattering Code ASA-100: Theory, Applications, Computer Code, and Listing," ASL-TR-0066, July 1980.
134. Sojka, Brian Z., and Kenneth J. White, "Evaluation of Specialized Photoacoustic Absorption Chambers for Near-Millimeter Wave (MMW) Propagation Measurements," ASL-TR-0067, August 1980.
135. Bruce, Charles W., Young Paul Yee, and S. G. Jennings, "In-Situ Measurement of the Ratio of Aerosol Absorption to Extinction Coefficient," ASL-TR-0068, August 1980.
136. Yee, Young Paul, Charles W. Bruce, and Ralph J. Brewer, "Gaseous/Particulate Absorption Studies at WSMR using Laser Sourced Spectrophones," ASL-TR-0069, June 1980.
137. Lindberg, James D., Raron B. Loveland, Melvin Heaps, James B. Gillespie, and Andrew F. Lewis, "Battlefield Dust and Atmospheric Characterization Measurements During West German Summertime Conditions in Support of Grafenwoehr Tests," ASL-TR-0066, September 1980.
138. Vechione, W. J., "Evaluation of the Environmental Instruments, Incorporated Series 200 Dual Component Wind Set," ASL-TR-0067, September 1980.
139. Bruce, C. W., Y. P. Yee, B. D. Hinds, R. G. Pinnick, R. J. Brewer, and J. Minjares, "Initial Field Measurements of Atmospheric Absorption at 9um to 11um Wavelengths," ASL-TR-0068, October 1980.
140. Heaps, M. G., R. O. Olsen, K. D. Baker, D. A. Burt, L. C. Howlett, L. L. Jensen, E. F. Pound, and G. D. Allred, "1979 Solar Eclipse: Part II Initial Results for Ionization Sources, Electron Density, and Minor Neutral Constituents," ASL-TR-0069, October 1980.
141. Low, Richard D. H., "One-Dimensional Cloud Microphysical Models for Central Europe and their Optical Properties," ASL-TR-0070, October 1980.

142. Duncan, Louis D., James D. Lindberg, and Radon B. Loveland, "An Empirical Model of the Vertical Structure of German Fogs," ASL-TR-0071, November 1980.
143. Duncan, Louis D., 1981, "EOSAEL 80, Volume I, Technical Documentation," ASL-TR-0072, January 1981.
144. Shirkey, R. C., and S. G. O'Brien, "EOSAEL 80, Volume II, Users Manual," ASL-TR-0073, January 1981.
145. Bruce, C. W., "Characterization of Aerosol Nonlinear Effects on a High-Power CO<sub>2</sub> Laser Beam," ASL-TR-0074, February 1981.
146. Duncan, Louis D., and James D. Lindberg, "Air Mass Considerations in Fog Optical Modeling," ASL-TR-0075, February 1981.
147. Kunkel, Kenneth E., "Evaluation of a Tethered Kite Anemometer," ASL-TR-0076, February 1981.
148. Kunkel, K. E., et al, "Characterization of Atmospheric Conditions at the High Energy Laser System Test Facility (HELSTF) White Sands Missile Range, New Mexico, August 1977 to October 1978, Part II, Optical Turbulence, Wind, Water Vapor Pressure, Temperature," ASL-TR-0077, February 1981.
149. Miers, Bruce T., "Weather Scenarios for Central Germany," ASL-TR-0078, February 1981.
150. Cogan, James L., "Sensitivity Analysis of a Mesoscale Moisture Model," ASL-TR-0079, March 1981.
151. Brewer, R. J., C. W. Bruce, and J. L. Mater, "Optoacoustic Spectroscopy of C<sub>2</sub>H<sub>6</sub> at the 9 $\mu$ m and 10 $\mu$ m C<sup>12</sup>O<sub>2</sub><sup>16</sup> Laser Wavelengths," ASL-TR-0080, March 1981.
152. Swingle, Donald M., "Reducible Errors in the Artillery Sound Ranging Solution, Part I: The Curvature Correction" (U), SECRET, ASL-TR-0081, April 1981.
153. Miller, Walter B., "The Existence and Implications of a Fundamental System of Linear Equations in Sound Ranging" (U), SECRET, ASL-TR-0082, April 1981.
154. Bruce, Dorothy, Charles W. Bruce, and Young Paul Yee, "Experimentally Determined Relationship Between Extinction and Liquid Water Content," ASL-TR-0083, April 1981.
155. Seagraves, Mary Ann, "Visible and Infrared Obscuration Effects of Ice Fog," ASL-TR-0084, May 1981.

156. Watkins, Wendell R., and Kenneth D. White, "Wedge Absorption Remote Sensor," ASL-TR-0085, May 1981.
157. Watkins, Wendell R., Kenneth D. White, and Laura J. Crow, "Turbulence Effects on Open Air Multipaths," ASL-TR-0086, May 1981.
158. Blanco, Abel J., "Extending Application of the Artillery Computer Meteorological Message," ASL-TR-0087, May 1981.
159. Heaps, M. G., D. W. Hoock, R. P. Oisen, R. F. Engebos, and R. Ratijo, "High Frequency Position Location: An Assessment of Current Status and Potential Improvements," ASL-TR-0088, May 1981.
160. Watkins, Wendell R., and Kenneth D. White, "Laboratory Facility for Measurement of Hot Gaseous Plume Radiative Transfer," ASL-TR-0089, June 1981.
161. Heaps, M. G., "Dust Cloud Models: Sensitivity of Calculated Transmittances to Variations in Input Parameters," ASL-TR-0090, June 1981.
162. Seagraves, Mary Ann, "Some Optical Properties of Blowing Snow," ASL-TR-0091, June 1981.
163. Kobayashi, Herbert K., "Effect of Hail, Snow, and Melting Hydrometeors on Millimeter Radio Waves," ASL-TR-0092, July 1981.
164. Cogan, James L., "Techniques for the Computation of Wind, Ceiling, and Extinction Coefficient Using Currently Acquired RPV Data," ASL-TR-0093, July 1981.
165. Miller, Walter B., and Bernard F. Engebos, "On the Possibility of Improved Estimates for Effective Wind and Temperature," (U), SECRET, ASL-TR-0094, August 1981.
166. Heaps, Melvin G., "The Effect of Ionospheric Variability on the Accuracy of High Frequency Position Location," ASL-TR-0095, August 1981.
167. Sutherland, Robert A., Donald W. Hoock, and Richard B. Gomez, "An Objective Summary of US Army Electro-Optical Modeling and Field Testing in an Obscuring Environment," ASL-TR-0096, October 1981.
168. Pinnick, R. G., et al, "Backscatter and Extinction in Water Clouds," ASL-TR-0097, October 1981.
169. Cole, Henry P., and Melvin G. Heaps, "Properties of Dust as an Electron and Ion Attachment Site for Use in D Region Ion Chemistry," ASL-TR-0098, October 1981.

